Accepted Manuscript

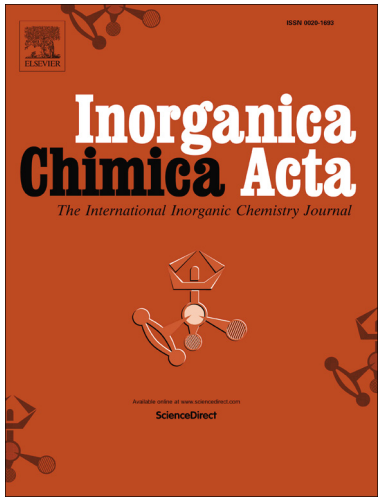

Research paper

Synthesis of 5-nitro-salicylaldehyde-N-substituted thiosemicarbazonates of copper(II) : Molecular structures, spectroscopy, ESI-mass studies and antimicrobial activity

Tarlok S. Lobana, Shikha Indoria, Henna Sood, Daljit S. Arora, Balwinder S. Randhawa, Isabel Garcia-Santos, Victoria A. Smolinski, Jerry P. Jasinski

PII: S0020-1693(17)30211-6
DOI: http://dx.doi.org/10.1016/j.ica.2017.02.032
Reference: ICA 17458

To appear in: *Inorganica Chimica Acta*

Received Date: 14 February 2017
Revised Date: 25 February 2017
Accepted Date: 27 February 2017

Please cite this article as: T.S. Lobana, S. Indoria, H. Sood, D.S. Arora, B.S. Randhawa, I. Garcia-Santos, V.A. Smolinski, J.P. Jasinski, Synthesis of 5-nitro-salicylaldehyde-N-substituted thiosemicarbazonates of copper(II) : Molecular structures, spectroscopy, ESI-mass studies and antimicrobial activity, *Inorganica Chimica Acta* (2017), doi: http://dx.doi.org/10.1016/j.ica.2017.02.032

This is a PDF file of an unedited manuscript that has been accepted for publication. As a service to our customers we are providing this early version of the manuscript. The manuscript will undergo copyediting, typesetting, and review of the resulting proof before it is published in its final form. Please note that during the production process errors may be discovered which could affect the content, and all legal disclaimers that apply to the journal pertain.

ACCEPTED MANUSCRIPT

Full paper

Synthesis of 5-nitro-salicylaldehyde-N-substituted thiosemicarbazonates of copper(II) : Molecular structures, spectroscopy, ESI-mass studies and antimicrobial activity

Tarlok S. Lobana,*[a] Shikha Indoria,[a] Henna Sood,[b] Daljit S. Arora,[b] Balwinder S. Randhawa,[a] Isabel Garcia-Santos,[c] Victoria A. Smolinski,[d] and Jerry P. Jasinski[d]

[a]*Department of Chemistry, Guru Nanak Dev University, Amritsar-143 005, India.*

[b]*Department of Microbiology, Guru Nanak Dev University, Amritsar-143 005, India*

[c]*Departamento de Quimica Inorganica, Facultad de Farmacia, Universidad de Santiago, 15782-Santiago, Spain*

[d]*Department of Chemistry, Keene State College, Keene, NH 03435 USA*

E-mail: tarlokslobana@yahoo.co.in (T.S. Lobana); Fax: 91-183-2258820

ABSTRACT

Equimolar reactions of copper(II) acetate with 5-nitro-salicylaldehyde-N^1-substituted thiosemi – carbazones, [5-NO_2-2-HO–C_6H_4-C^2(H)=N^3–N^2H–C^1(=S)–N^1HR; R = Me, H_2L-NHMe; Et, H_2L-NHEt; Ph, H_2L-NHPh; H, H_2L-NH_2], and 4, 4'-dimethyl-2,2'-bipyridine (dm-bipy), 2, 9-dimethyl-1, 10-phenanthroline (dm-phen) and 3, 4, 7, 8-tetramethyl-1,10-phenanthroline (tm-phen) have yielded complexes of stoichiometry, [Cu(κ^3-O,N,S-5-NO_2-stscN^1HR)(κ^2-N,N-L')] {R = H (**1**, **2**, **3**), Me (**4**, **5**, **6**), Et(**7**, **8**, **9**), Ph (**10**, **11**, **12**); L'= dm-bipy (**1**, **4**, **7**, **10**) / dm-phen (**2**, **5**, **8**, **11**) / tm-phen (**3**, **6**, **9**, **12**)}. They have been investigated by analytical data, infrared and electronic absorption spectroscopy, electron spin resonance spectroscopy, fluorescence activity, ESI-mass study and single crystal X-ray crystallography (**1**, **6**, **7**). The geometry of complexes is slightly distorted square pyramidal and have displayed weak to intense fluorescence in the region, 370-570 nm. Complexes have shown significant antimicrobial activity against methicillin resistant *Staphylococcus aureus* (MRSA), *Staphylococcus aureus* (MTCC740), *Klebsiella*

ACCEPTED MANUSCRIPT

pneumoniae (MTCC109), *Shigella flexneri* (MTCC1457), *Salmonella typhimurium* (MTCC-439), and *Candida albicans* (MTCC227). Complexes are cytotoxic against living cells and thus they are bactericidal / fungicidal.

Keywords: 5-nitro-salicylaldehyde-N^1-substituted thiosemicarbazones; 4, 4'-dimethyl-2,2'-bipyridine, 2,9-dimethyl-1, 10-phenanthroline, copper(II), antimicrobial activity

1. Introduction

Study of the coordination chemistry of thiosemicarbazones (Chart 1, structure I and analogous ligands) describes molecular structures, variable nuclearity, cyclometallation, catalysis, analytical chemistry and finally the biochemical applications of metal complexes which comprise the chief interest of several scientists [1-17]. Biological applications of metal thiosemicarbazones reported in the literature pertain to in vitro molecular imaging devices, anticancer activity, inhibition of DNA and RNA synthesis, disruption of ATP production, neuroprotective activity in cell and animal models of Alzheimer's disease (AD), antimicrobial activity, anti-tumor activity and cytotoxicity [18-51].

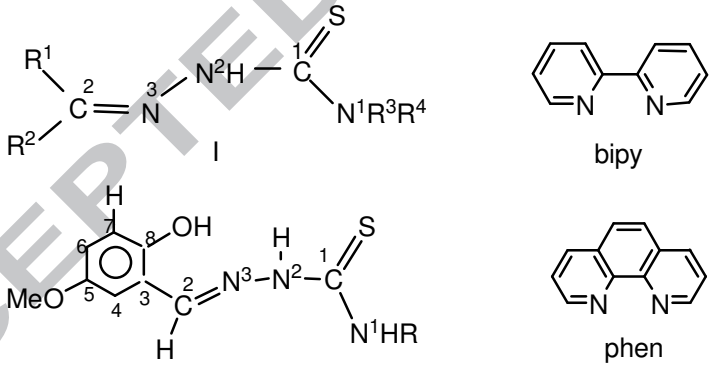

Chart 1. Thiosemicarbazones and col-ligands

Regarding the biochemical status of metal derivatives of salicylaldehyde based thiosemicarbazones, these complexes exhibited antitumor activity [37, 42], photo-induced DNA cleavage [43] and antimicrobial activity [44-51]. In order to develop metallo-organic antimicrobial agents, we have recently reported [18] antimicrobial activity of complexes of

ACCEPTED MANUSCRIPT

copper(II)/zinc(II) with salicylaldehyde based thiosemicarbazones (Charts 1 and 2) for methoxy and/or nitro groups at the 5-position in structure II with bipy, phen, dm-phen and tm-phen co-ligands[18, 52-54]. These complexes showed significant growth inhibitory activity (antimicrobial activity) against methicillin resistant *Staphylococcus aureus* (MRSA), *Staphylococcus aureus*, *Klebsiella pneumoniae*, *Shigella flexneri* and *Candida albicans*.

In continuation, in this paper, 5-nitro-salicyaldehyde-N^1-substituted thiosemicarbazones and 4, 4'-dimethyl-2,2'-bipyridine (dm-bipy), 2,9-dimethyl-1,10-phenanthroline (dm-phen) and 3, 4, 7, 8-tetramethyl-1,10-phenanthroline (tm-phen) ligands have been used for the synthesis of copper(II) complexes (Chart 2). Here, the main objective of the study was to investigate the effect of substituents in the pyridine rings of 2,2'-bipyridine / 1,10-phenanthroline on antimicrobial activity.

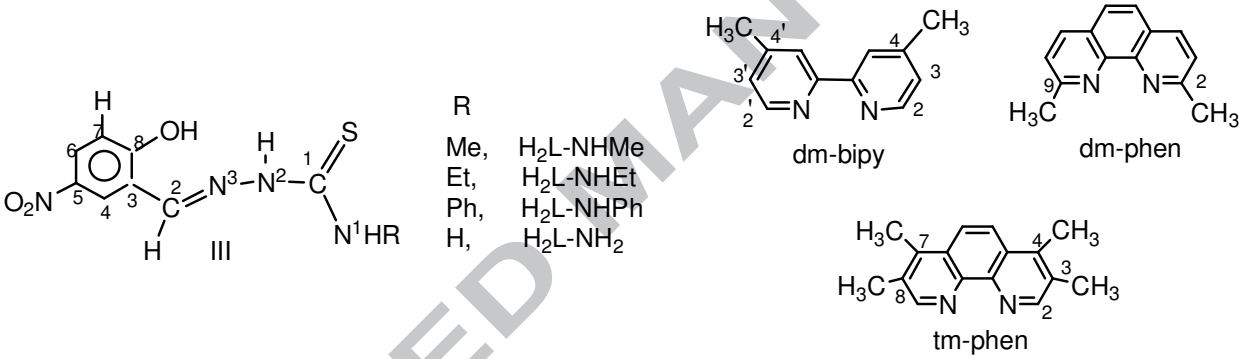

Chart 2. Salicylaldehyde thiosemicarbazones and co-ligands used in the present study.

2. Experimental

Copper(II) acetate monohydrate, thiosemicarbazide, N-methylthiosemicarbazide, N-ethylthio- semicarbazide, N-phenylthiosemicarbazide, 5-nitro-salicylaldehyde, 4, 4′-dimethyl-2,2-bipyridine (dm-bipy), 2, 9-dimethyl-1,10-phenanthroline (dm-phen) and 3,4,7,8-tetramethyl-1,10-phenanthroline (tm-phen) were procured from Aldrich Sigma Ltd. The thio-ligands (Chart 2) were prepared as reported earlier [18, 52-54]. Elemental analysis for C, H, and N were carried out with a thermoelectron FLASHEA1112 analyzer. Melting points were determined with a Gallenkamp electrically heated apparatus. IR spectra of the compounds were recorded in the 4000 – 450 cm^{-1}region with a Perkin Elmer FT-IR Spectrometer by making their KBr pellets.

ACCEPTED MANUSCRIPT

UV-visible spectra of the compounds (10^{-3}-10^{-4} M) were recorded in dimethylsulfoxide (dmso) with the help of a UV-1601 PC Shimadzu spectrophotometer. Fluorescence spectra of the complexes (10^{-4} M) were recorded with a Varian Cary Eclipse Fluorescence spectrophotometer. The ESI-mass spectra were recorded in DMSO using a Bruker Daltonik LS-MS high resolution microTOF-Q II 10356 spectrometer.

2.1. Synthesis of complexes

2.1.1. [*Cu(κ^3:O,N^3,S-5-NO_2-stsc-N^1H_2)(κ^2:N,N-dm-bipy)] (**1**).* To a pale yellow solution of thio-ligand 5-NO_2-H_2stsc-N^1H_2 (0.029 g, 0.127 mmol) in methanol (15 mL) was added dark green solid $Cu(OAc)_2 \cdot H_2O$ (0.025 g, 0.125 mmol) which led to the formation of light brown compound which was suspended in a mixture of dichloromethane and methanol (3 : 1 v/v) followed by the addition of solid dm-bipy (0.017 g, 0.125 mmol) and the contents were stirred for 15 min until a clear dark green solution was formed. The dark green solution was allowed to evaporate at room temperature which gave dark green crystals which were grown over a period of 10 days. Yield: 0.036 g, 75%, m.p. 205°C. *Anal.* Calc. for $C_{20}H_{18}CuN_6O_3S$: C 49.43; H 3.73; N 17.29; S 6.60; Found: C 49.52; H 3.49; N 17.46; S 6.39 %. IR (cm^{-1} , KBr): ν(N^1–H) 3390 w, ν(C–H) 3100 w, 2950 w; ν(C=N) + ν(C=C) + δ(N–H) 1598 s, ν(N=O) 1548 m, δ(C–H) 1489 s, 1470 w; 1380 m, δ(N=O) 1307 s; other bands, 1244 m, 1150 w, 1100 m, 947 w, 831 s; 805 s; ν(C–S) 784 s; other bands, 726 s, 652 s, 623 s. Electronic absorption spectrum (DMSO, λ_{max} /nm, ε / L mol^{-1} cm^{-1}): [10^{-3} M] 595 (1.85 x 10^2); [10^{-4} M] 394 (1.42 x 10^4), 333 (1.26 x 10^4), 280 (1.78 x 10^4). Fluorescence spectrum: (λ_{max}^{ex} = 320 nm; λ_{max}^{em} = 433 nm). ESI mass data: calc for $C_{20}H_{18}CuN_6O_3S$+H, [Cu(5-NO_2-stsc-N^1H_2)(dm-bipy) + H]$^+$ 486.40; obsd. m/z = 486.05. Complexes **2-12** were prepared by a similar method.

*2.1.2. [Cu(κ^3:O,N^3,S-5-NO_2-stsc-N^1H_2)(κ^2:N,N-dm-phen)] (**2**).* Yield: 0.035 g, 74%, m.p. 238°C. *Anal.* Calc. for $C_{22}H_{18}CuN_6O_3S$: C 51.81; H 3.56; N 16.48; S 6.29 %; Found: C 51.09; H 3.63; N 16.21; S 6.41 %. IR (cm^{-1} , KBr): ν(N^1–H) 3353 w; ν(C–H) 3170 w, 3000 w, 2985 w, ν(C=N) + ν(C=C) + δ(N–H) 1659 m, 1598 s; ν(N=O) 1549 s, δ(C–H) 1500 s, 1442 s; 1370 w, δ(N=O) 1314 s; other bands, 1220 s, 1153 w, 1100 s, 944 s, 861 w; ν(C–S) 763 s; other bands, 653 s, 626 s. Electronic absorption spectrum, (DMSO, λ_{max} /nm, ε / L mol^{-1} cm^{-1}): [10^{-3} M] 594 (2.24 x 10^2); [10^{-4} M] 406 (9.23 x 10^3), 332(8.51 x 10^3), 275 (1.88 x 10^4). Fluorescence spectrum: (λ_{max}^{em} = 434 nm;

ACCEPTED MANUSCRIPT

λ_{max}^{ex} = 320 nm). ESI mass data : calc. for $C_{22}H_{18}CuN_6O_3S$ +H, [Cu(5-NO_2-stsc-N^1H_2)(dm-phen) + H]$^+$, m/z = 510.05; obsd. m/z = 510.04.dm

*2.1.3. [Cu(κ^3:O,N^3,S-5-NO_2-stsc-N^1H_2)(κ^2:N,N-tm-phen)]·CH_3OH (**3**).* Yield: 0.037 g, 76%, m.p. 234°C. *Anal.* Calc. for $C_{24}H_{22}CuN_6O_3S·CH_3OH$: C 52.67; H 4.60; N 14.74; S 5.62 %; Found: C 52.09; H 4.90; N 15.01; S 6.01 %. IR (cm^{-1} , KBr): ν(N^1–H) 3420 w, ν(O–H)$_{CH3OH}$ 3390 w, ν(C–H) 3139 w, 3020 w; ν(C=N) + ν(C=C) + δ(N−H) 1610 s, 1595 s, ν(N=O) 1548 s, δ(C–H) 1484 s, 1470 s, 1429 s; 1380 m, 1350 m, δ(N=O) 1306 s, 1242 m, 1160 w, 1100 m, 947 w, 831 s, 805 s; ν(C–S) 784 s; 726 s, 652 s, 623 s. Electronic absorption spectrum, (DMSO, λ_{max} /nm, ε / L mol^{-1} cm^{-1}): [10^{-3} M] 590 (1.61 x 10^2); [10^{-4} M] 402 (1.18 x 10^4), 331 (9.84 x 10^3), 276 (2.58 x 10^4). Fluorescence spectrum: (λ_{max}^{em} = 436 nm; λ_{max}^{ex} = 320 nm). ESI mass data: calc. for $C_{24}H_{22}CuN_6O_3S·CH_3OH$ +H, [Cu(5-NO_2-stsc-N^1H_2)(tm-phen).CH_3OH + H]$^+$, m/z = 570.11; obsd. m/z = 570.16.

*2.1.4. [Cu(κ^3:O,N^3,S-5-NO_2-stsc-N^1HMe)(κ^2:N,N-dm-bipy)] (**4**).* Yield: 0.037 g, 74%, m.p. 223 °C. *Anal.* Calc. for $C_{21}H_{20}CuN_6O_3S$: C 50.44; H 4.03; N 16.81; S 6.41 %; Found: C 50.32; H 4.29; N 16.72; S 6.30 %. IR (cm^{-1} , KBr): ν(N^1–H) 3373 s; ν(C–H) 3130 w, 2990 w, 2970 w, 2887 w; ν(C=N) + ν(C=C) + δ(N-H) 1598 s, ν(N=O) 1547 m; δ(C-H) 1500 s, 1434 s, 1403 m; δ(N=O) 1302 s; other bands, 1099 w; 829 w, ν(C–S) 766 s; 516 w. Electronic absorption spectrum, (DMSO, λ_{max} /nm, ε / L mol^{-1} cm^{-1}): [10^{-3} M] 594 (2.28 x 10^2); [10^{-4} M] 394 (2.35 x 10^4), 332 (2.00 x 10^4), 283 (2.81 x 10^4). Fluorescence spectrum : (λ_{max}^{em} = 436 nm; λ_{max}^{ex} = 320 nm). ESI mass data: calc. for $C_{21}H_{20}CuN_6O_3S$+H, [Cu(5-NO_2-stsc-N^1HMe)(dm-bipy) + H]$^+$, m/z = 500.06; obsd. m/z = 500.05.

*2.1.5. [Cu(κ^3:O,N^3,S-5-NO_2-stsc-N^1HMe)(κ^2:N,N-dm-phen)] (**5**).* Yield: 0.039 g, 74%, m.p. 205 °C. *Anal.* Calc. for $C_{23}H_{20}CuN_6O_3S$: C 52.71; H 3.85; N 16.04, S 6.12 %.; Found: C 52.43; H 3.65; N 15.83, S 6.37 %. IR (cm^{-1} , KBr): ν(N^1–H) 3382 w; ν(C–H) 3090 w, 3004 w, 2888 w; ν(C=N) + ν(C=C) + δ(N−H) 1608 s, 1581 s; ν(N=O) 1550 w; δ(C−H) 1491 s; δ(N=O) 1307 s; 1036 s, 830 s; ν(C–S) 769 s; 517 w. Electronic absorption spectrum, (DMSO, λ_{max} /nm, ε / L mol^{-1} cm^{-1}): [10^{-3} M] 585 (2.54 x 10^2); [10^{-4} M] 399 (7.79 x 10^3), 324 (6.93 x 10^3), 284 (1.85 x 10^4). Fluorescence spectrum: (λ_{max}^{em} = 434 nm; λ_{max}^{ex} = 320 nm). ESI mass data : calc. for $C_{23}H_{20}CuN_6O_3S$+H, [Cu(5-NO_2-stsc-N^1HMe)(dm-phen) + H]$^+$ 524.07; obsd. m/z = 524.08.

ACCEPTED MANUSCRIPT

*2.1.6. [Cu(κ^3:O,N^3,S-5-NO_2-stsc-N^1HMe)(κ^2: N, N-tm-phen)]·H_2O (**6**).* Yield: 0.041 g, 73%, m.p. 243°C. *Anal.* Calc. for $C_{25}H_{24}CuN_6O_3S·H_2O$: C 52.67; H 4.60; N 14.74, S 5.62 %; Found: C 52.81; H 4.77; N 15.06, S 5.29 %. IR (cm^{-1} , KBr): ν(N^1–H) + ν(O–H)$_{H2O}$ 3442 br; ν(C–H) 3048 w, 2937 w, 2889 w; ν(C=N) + ν(C=C) + δ(N−H) 1597 s, ν(N=O) 1548 m; 1504 m δ(C−H) 1492 s, 1432 s; 1369 m; δ(N=O) 1308 s; 1242 m, 1192 w, 1146 w, 1102 s, 1069 w, 1011 w, 953 m, 884 m; 819 s; ν(C–S) 729 s; 698 m, 651 m, 619 w, 514 w, 468 w. Electronic absorption spectrum, (DMSO, λ_{max} /nm, ε / L mol^{-1} cm^{-1}): [10^{-3} M] 589 (1.90 x 10^2); [10^{-4} M] 402 (1.44 x 10^4), 330 (1.29 x 10^4), 276 (3.59 x 10^4). Fluorescence spectrum: (λ_{max}^{em} = 435 nm; λ_{max}^{ex} = 320 nm). ESI mass data: calc. for $C_{25}H_{24}CuN_6O_3S·H_2O$+H, [Cu(5-$NO_2$-stsc-$N^1$HMe)(tm-phen).$H_2O$ + H]$^+$ 570.11; obsd. m/z = 570.18. The crystals were formed after recrystallisation in CH_2Cl_2 and MeOH. X-ray showed the presence of CH_2Cl_2.

*2.1.7. [Cu(κ^3:O,N^3,S-5-NO_2-stsc-N^1HEt)(κ^2:N,N-dm-bipy)]·CH_2Cl_2 (**7**).* Yield: 0.036 g, 71 %, m.p. 208 °C. *Anal.* Calc. for $C_{22}H_{22}CuN_6O_3S·CH_2Cl_2$: C 46.12; H 4.04; N 14.03; S 5.35 %; Found: C 45.94; H 4.33; N 14.41; S 5.72 %. IR (cm^{-1} , KBr): ν(N^1–H) 3386 w; ν(C–H) 3145 m, 3056 w, 2880 w; ν(C=N) + ν(C=C) + δ(N−H) 1598 s; ν(N=O) 1549 s; δ(C−H) 1493 s, 1458 w; δ(N=O) 1308 s; 1244 s, 1150 w, 1100 s, 1026 w, 829 w; ν(C–S) 763 s; 427 w. Electronic absorption spectrum, (DMSO, λ_{max} /nm, ε / L mol^{-1} cm^{-1}): [10^{-3} M] 592 (2.47 x 10^2); [10^{-4} M] 398 (2.26 x 10^4), 333 (1.89 x 10^4), 287 (2.30 x 10^4). Fluorescence spectrum: (λ_{max}^{em} = 440 nm; λ_{max}^{ex} = 320 nm). ESI mass data: calc. for $C_{22}H_{22}CuN_6O_3S$+H, [Cu(5-NO_2-stsc-N^1HEt)(dm-bipy) + H]$^+$ 514.08; obsd. m/z = 514.45.

*2.1.8. [Cu(κ^3-O,N^3,S-5-NO_2-stsc-N^1HEt)(κ^2-N,N-dm-phen)] (**8**).* Yield: 0.039 g, 74 %, m.p. 195°C. *Anal.* Calc. for $C_{24}H_{22}CuN_6O_3S$: C 53.57; H 4.12; N 15.62; S 6.00 %; Found: C 53.02; H 4.33; N 15.03; S 5.95 %. IR (cm^{-1} , KBr): ν(N^1–H) 3390 s, ν(C–H) 3060 w, 2968 w, 2930 w, 2880 w; ν(C=N) + ν(C=C) + δ(N−H) 1597 s; ν(N=O) 1549 s; δ(C–H) 1501 s, 1430 s; 1397 m, δ(N=O) 1313 s; 1242 w, 1192 w, 1151 w, 1100 m, 937 w, 858 m, 826 w; ν(C–S) 758 s; 652 m, 513 w. Electronic absorption spectrum, (DMSO, λ_{max} /nm, ε / L mol^{-1} cm^{-1}): [10^{-3} M] 605 (2.58 x 10^2); [10^{-4} M] 402 (2.27 x 10^4), 332 (1.84 x 10^4), 296 (2.55 x 10^4), 277 (3.80 x 10^4). Fluorescence spectrum: (λ_{max}^{em} = 436 nm; λ_{max}^{ex} = 320 nm).

ACCEPTED MANUSCRIPT

2.1.9. [Cu(κ^3:O,N,S-5-NO_2-stsc-N^1HEt)(κ^2:N,N-tm-phen)] ***(9)***. Yield: 0.042 g, 74%, m.p. 199°C. *Anal.* Calc. for $C_{26}H_{26}CuN_6O_3S$: C 55.16; H 4.63; N 14.84; S 5.66 %; Found: C 54.89; H 4.21; N 15.09; S 5.76 %. IR (cm^{-1} , KBr): ν(N^1–H) 3345 s, ν(C–H) 3100 w, 3055 w, 2969 w, 2880 w; ν(C=N) + ν(C=C) + δ(N−H) 1601 s; ν(N=O) 1549 s; δ(C–H) 1488 s, 1467 s, 1431 s; 1372 m, δ(N=O) 1310 s; 1240 m, 1194 s, 1147 m, 938 w; 826 s; ν(C–S) 726 m; 697 m, 655 m, 515 w. Electronic absorption spectrum, (DMSO, λ_{max} /nm, ε / L mol^{-1} cm^{-1}): [10^{-3} M] 590 (2.8 x 10^2); [10^{-4} M] 406 (2.69 x 10^4), 332 (2.63 x 10^4), 266 (3.95 x 10^4). Fluorescence spectrum: (λ_{max}^{em} = 439 nm; λ_{max}^{ex} = 320 nm). ESI mass data: calc. for $C_{26}H_{26}CuN_6O_3S$+H, [Cu(5-NO_2-stsc-N^1HEt)(tm-phen)+H]$^+$, m/z = 566.12; obsd. m/z = 566.13.

2.1.10. [Cu(κ^3:O,N,S-5-NO_2-stsc-N^1HPh)(κ^2: N,N-dm-bipy)] ***(10)***. Yield: 0.039 g, 71 %, m.p. 226°C. *Anal.* Calc. for $C_{26}H_{22}CuN_6O_3S$: C 55.56; H 3.94; N 14.95;S 5.70 %; Found: C 56.01; H 3.63; N 14.73; S 5.45 %. IR (cm^{-1} , KBr): ν(N^1–H) 3386 s, ν(C–H) 3145 w, 3057 m, 2858 w; ν(C=N) + ν(C=C) + δ(N−H) 1598 s; ν(N=O) 1549 s; δ(C–H) 1493 s, 1470 w; 1375 w; δ(N=O) 1308 s; 1244 m, 1149 w, 1100 m, 948 w, 829 s; ν(C–S) 757 s; 692 w, 567 w, 427 w. Electronic absorption spectrum, (DMSO, λ_{max} /nm, ε / L mol^{-1} cm^{-1}): [10^{-3} M] 593 (2.25 x 10^2); [10^{-4} M] 394 (2.08 x 10^4), 332 (2.79 x 10^4), 283 (2.69 x 10^4). Fluorescence spectrum: (λ_{max}^{em} = 438 nm; λ_{max}^{ex} = 320 nm). ESI mass data: calc. for $C_{26}H_{22}CuN_6O_3S$ +H, [Cu(5-NO_2- stsc-N^1HPh)(dm-bipy) + H]$^+$ 562.08; obsd. m/z = 562.69.

2.1.11. [Cu(κ^3:O,N,S-5-NO_2-stsc-N^1HPh)(κ^2:dm-phen)] ***(11)***. Yield: 0.041 g, 75 %, m.p. 201°C. *Anal.* Calc. for $C_{28}H_{22}CuN_6O_3S{\cdot}CH_2Cl_2$: C 57.38; H 3.78; N 14.34;S 5.47 %; Found: C 56.82; H 4.13; N 14.29; S 5.79 %. IR (cm^{-1} , KBr): ν(N^1–H) 3314 s, ν(C–H) 2995 w, 2881 w; ν(C=N) + ν(C=C) + δ(N−H) 1608 s; ν(N=O) 1548 w; δ(C-H) 1509 s, 1470 w; 1375 w; δ(N=O) 1313 s; 1243 w, 1100 m, 943 w, 829 s; ν(C–S) 761 s; 656 m, 574 w, 427 w. Electronic absorption spectrum, (DMSO, λ_{max} /nm, ε / L mol^{-1} cm^{-1}): [10^{-3} M] 595 (2.25 x 10^2); [10^{-4} M] 398(1.89 x 10^4), 332 (2.50 x 10^4), 291 (2.58 x 10^4), 277 (3.68 x 10^4). Fluorescence spectrum: (λ_{max}^{em} = 436 nm; λ_{max}^{ex} = 320 nm). ESI mass data: calc. for $C_{28}H_{22}CuN_6O_3S{\cdot}CH_2Cl_2$+H, [Cu(5-$NO_2$-stsc-$N^1$ HPh)(dm-phen).CH_2Cl_2 + H]$^+$, m/z = 670.03; obsd. m/z = 670.01.

ACCEPTED MANUSCRIPT

2.1.12. [Cu(κ^3:O,N^3,S-5-NO_2- stsc-N^1HPh)(κ^2:N,N-tm-phen)] ***(12)***. Yield: 0.042 g, 75%, m.p. 198°C. *Anal.* Calc. for $C_{30}H_{26}CuN_6O_3S$: C 58.67; H 4.27; N 13.68; S 5.22 %; Found: C 59.01; H 4.36; N 13.58; S 5.38 %. IR (cm^{-1} , KBr): ν(N^1–H) 3384 s, ν(C–H) 3143 br, 3056 m, 2899 w; ν(C=N) + ν(C=C) + δ(N−H) 1598 s; ν(N=O) 1548 s; δ(C-H) 1487 s, 1487 s; 1374 m; δ(N=O) 1306 s; 1244 m, 1197 w, 1149 w, 1099 s, 948 w, 828 s, ν(C–S) 755 m; 680 w, 653 w, 624 w, 516 w, 420 w. Electronic absorption spectrum, (DMSO, λ_{max} /nm, ε / L $mol^{-1}cm^{-1}$) : [10^{-3} M] 591 (2.33 x 10^2), [10^{-3} M] 396 (1.97 x 10^4), 332 (2.03 x 10^4), 276 (3.77 x 10^4). Fluorescence spectrum: (λ_{max}^{em} = 437 nm; λ^{ex} = 320 nm).

2.2. X-ray crystallography

The crystal structures of complexes **1**, **6** and **7** were determined by mounting a single crystal of a complex on a glass fiber and data were measured with an Agilent Eos, Gemini diffractometer, equipped with graphite monochromated Mo-Kα (λ = 0.71073 Å) radiation at 173(2) K. The structures were solved by direct methods and refined using full-matrix least-squares techniques based on F^2 using ShelXL-2014. In these structures, all non-hydrogen atoms were refined anisotropically and the hydrogens have been fixed geometrically [55-60].

3. Results and discussion

3.1. Synthesis and IR spectroscopy

Chart 3 shows the formation of copper(II) complexes from 5-nitro-salicylaldehyde-N^1-substituted thiosemicarbazones and N, N-donor co-ligands. During reaction of $Cu(OAc)_2(H_2O)$ with a thiosemicarbazone ligand, both -2-OH and –N^2-H protons were removed by the acetate base and the thio-ligand as a dianion bonded to Cu^{II} to form a {Cu(O,N,S-L)} moiety which was treated with N,N-donor heterocyclic Lewis bases, namely, dm-bipy, dm-phen and tm–phen giving rise to the formation of dark green copper(II) complexes, [Cu(κ^3-O,N,S-5-NO_2-stscN^1HR)(κ^2-N,N-L')] **1-12.** These complexes are soluble in dichloromethane, methanol, acetonitrile and dimethyl sulfoxide and are stable to moisture and air.

ACCEPTED MANUSCRIPT

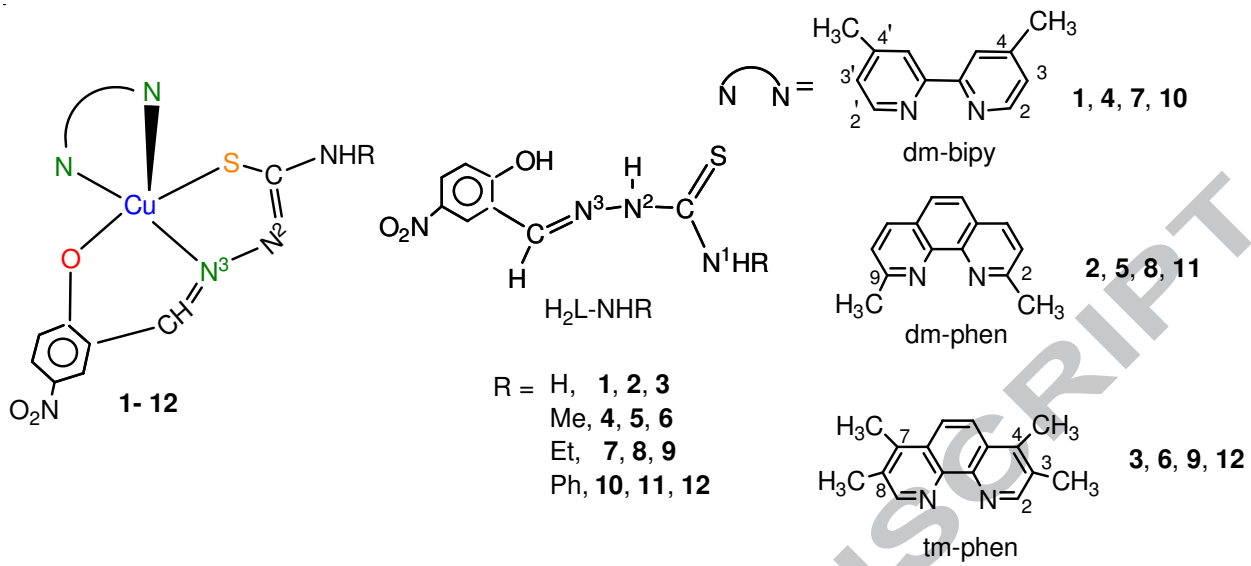

Chart 3. Thio-ligands and co-ligands in the formation of complexes **1**-**12**.

IR spectra of the copper(II) complexes shows the absence of diagnostic ν(O–H) and ν(N^2–H) bands which support that the thio-ligands (H_2L-NHR) are coordinating as dianions (L-NHR)$^{2-}$. In a typical example, the IR spectrum of the H_2L-NH_2 ligand showed vibrational bands due to ν(N^2–H) and ν(O–H) as a broad band at 3221 cm^{-1}. This broad band was found to be absent in its complex, [Cu(κ^3:O,N^3,S-5-NO_2-stsc-N^1H_2)(κ^2:N,N-dm-bipy)] **1**, which suggested deprotonation of both (N^2–H) and (O–H) moieties and thus allowing thio-ligand binding to the metal as a dianion. The ν(N^1–H) vibrational band of the –N^1HR moiety appeared at 3390 cm^{-1} in complex **1**. The aromatic ring at the C^2 carbon showed a ν(C–H) band at 3059 cm^{-1} and a methyl group at N^1 atom showed ν(C–H) bands at 3100 and 2950 cm^{-1}. The nitro group (–NO_2) present in the aromatic ring showed a ν(N-O) stretching band at 1548 and and δ(N-O) at 1307 cm^{-1}. The diagnostic ν(C=S) band of the free ligand at 845 cm^{-1} shifted to low energy at 784 cm^{-1} in complex **1** [52, 61-65]. The bands due to the ν(C=N), ν(C=C) , δ(N–H) and δ(C–H) vibrational modes are listed in the experimental section. Complexes **2-12** showed similar trends in these vibrational bands (see experimental).

ACCEPTED MANUSCRIPT

3.2. Crystal and molecular structures

Complexes, [Cu(κ^3-O, N^3, S-5-NO_2-stsc-N^1H_2)(κ^2-N, N-dm-bipy)] **1,** [Cu(κ^3-O, N^3, S-5-NO_2-stsc-N^1HMe)(κ^2-N, N-tm-phen)] **6**, and [Cu(κ^3-O, N^3, S-5-NO_2-stsc-N^1HEt)(κ^2-N, N-dm-bipy)] **7** gave single crystals while others did not yield crystals suitable for single crystal X-ray crystallography. Complexes **1**, **6** and **7** crystallized in orthorhombic, triclinic and monoclinic crystal systems in space groups Pccn, P$\bar{1}$ and C_2/c, respectively. The crystal data are placed in Table 1, while Table 2 gives important bond parameters.

The molecular structure of complex **1** is shown in Fig. 1. In this complex, copper(II) is coordinated to O, N, S donor atoms of the thio-ligand and two nitrogen atoms, $N4_{(eq)}$ and $N5_{(ax)}$ of the 4, 4′-Me_2-bipy co-ligand, (N_{eq} - equatorial nitrogen, N_{ax} - axial nitrogen). The O(1), N(1), S(1) and $N4_{(eq)}$ atoms occupy a square plane while the $N5_{(ax)}$ nitrogen atom occupies one axial site. The *trans* bond angles in the square plane, namely, O-Cu-S, 151.13(6) and N3-Cu-176.86(8)(N4) as well as the adjacent bond angles in the range, ca. 83-96°, reveal a distorted square pyramid geometry. It is also added here that the distortion value of a coordination polyhedron, $\tau = (\beta-\alpha)/60$, is evaluated by the two largest bond angles in five coordination geometry (τ = 1 for ideal trigonal bipyramid and 0 for square pyramidal environment) [66], and this value (τ) is equal to 0.428 for complex **1**, which is slightly more than that found in analogous unsubstituted bipy Cu^{II} complex (τ = 0.34) [52]. Another complex [Cu(κ^3-O, N^3, S-5-NO_2-stsc-N^1HEt)(κ^2-N, N-dm-bipy)] **7** with an ethyl substitution at N^1 nitrogen has a similar structure, and bond parameters and the τ value = 0.407 (Fig. 2).

The coordination pattern of tm-phen complex, [Cu(κ^3-O, N^3, S-5-NO_2-stsc-N^1HMe)(κ^2-N, N-tm-phen)] **6 (Fig. 3),** is similar to that of complex **1** except for the difference in the bond angles, O1-Cu-S1, 164.70(6)° and N-Cu- $N5_{(eq)}$, 172.53(8), which gives rise to a low value of τ = 0.131. It suggests that the geometry of complex is more closely related to a regular square pyramid. It may be due to the rigidity of phen ring with lesser coordination flexibility unlike the dm-bipy complexes **1** and **6** above, which formed distorted square pyramidal complexes. This trend is in line with a related phen complex, [Cu(5-NO_2-stsc-NHEt)(phen)] (τ = 0.132) [52].

ACCEPTED MANUSCRIPT

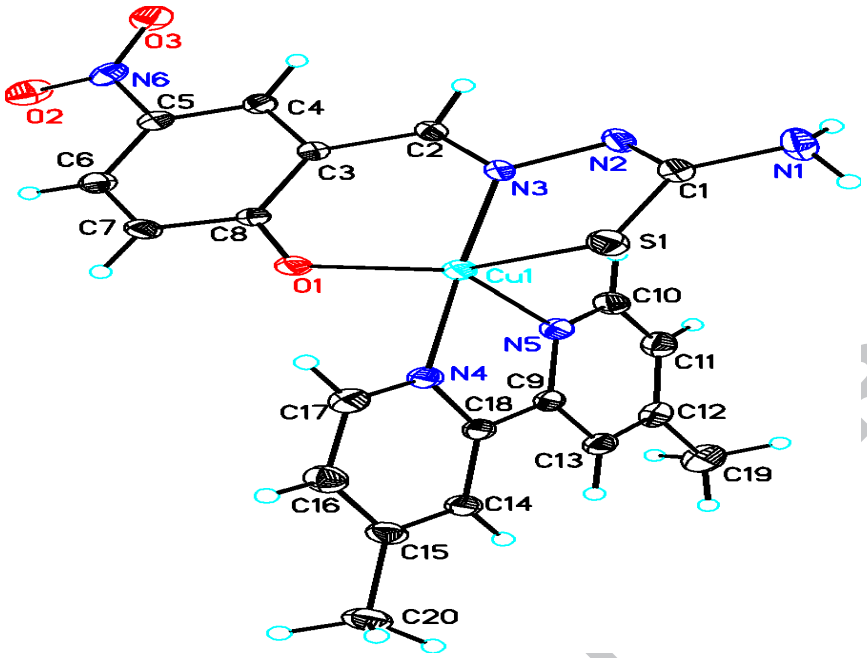

Fig. 1. Molecular structure of complex, [Cu(κ^3-O,N^3,S-5-NO_2-stsc-N^{1}H$_2$)(κ^2-N, N-dm-bipy] (**1**) showing the atom numbering scheme and 30% probability ellipsoids.

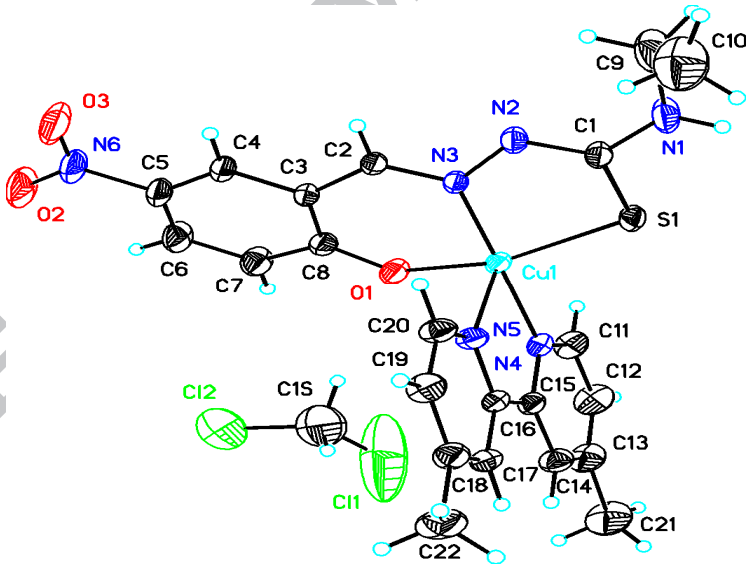

Fig. 2. Molecular structure of [Cu(κ^3-O,N^3,S-5-NO_2-stsc-N^{1}HEt)(κ^2-N,N-dm-bipy]·CH_2Cl_2 (**7**) showing the atom numbering scheme and 30% probability ellipsoids.

ACCEPTED MANUSCRIPT

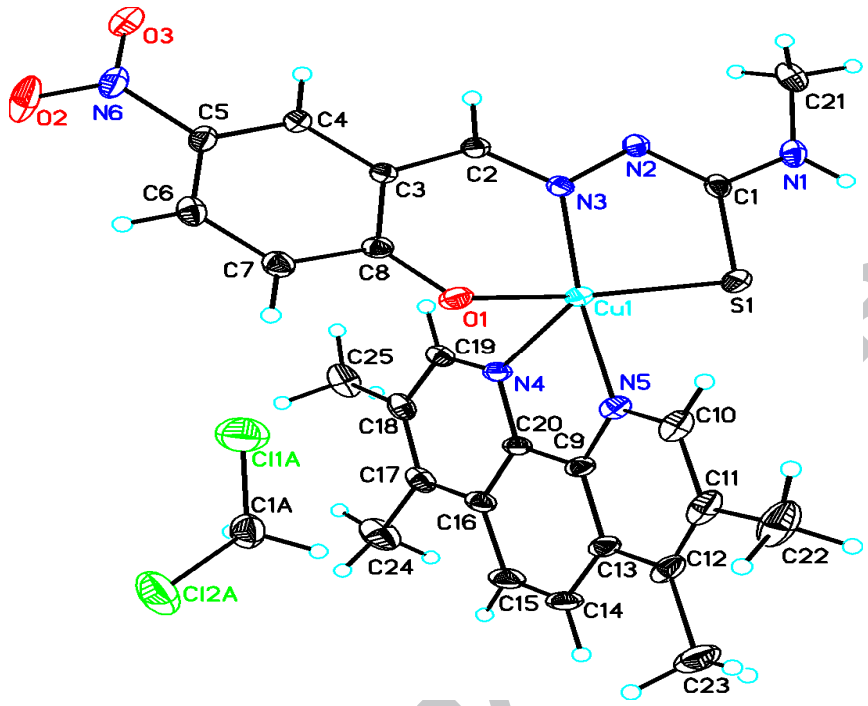

Fig. 3. Molecular structure of [Cu(κ^3-O,N^3,S-5-NO_2-stsc-N^{1}HMe)(κ^2-N, N-tm-phen]·CH_2Cl_2 (**6**) showing the atom numbering scheme and 30% probability ellipsoids.

Table 1

Crystallographic data for complexes **1**, **6** and **7**.

Compound	**1** (H)	**6**(Me)	**7** (Et)
Chemical formula	$C_{20}H_{18}CuN_6O_3S$	$C_{25}H_{24}CuN_6O_3S$, CH_2Cl_2	$C_{22}H_{22}CuN_6O$, CH_2Cl_2
M	486.00	637.03	598.98
T(K)	173(2)	173(2)	173(2)
Crystal system	Orthorhombic	Triclinic	Monoclinic
Space group	Pccn	$P\bar{1}$	C_2/c
Unit cell dimensions			
a(Å)	18.6471(3)	9.2150(8)	23.4042(7)

ACCEPTED MANUSCRIPT

b(Å)	18.3166(3)	10.8294(6)	11.0202(4)
c(Å)	12.5820(2)	13.9755(8)	20.2999(6)
α(°)	90	84.161(5)	90
β(°)	90	88.599(6)	100.273(3)
γ(°)	90	73.670(6)	90
V(Å^3)	4297.40(13)	1331.44(16)	5151.8(3)
Z	8	2	8
D_{calcd}(g cm^{-3})	1.502	1.589	1.545
μ(mm^{-1})	1.148	1.141	1.174
F(000)	1992	654	2456
Reflections collected	69707	16506	19270
Unique reflections	7573 (R_{int} = 0.0488)	8760, (R_{int} = 0.0350)	8535, (R_{int} = 0.0292)
Data/restraints/ parameters	7573/ 0/283	8760/0/357	8535/0/328
Reflens.with [I>2σ(I)]	5423	6734	6099
R Indices			
R_1	0.0503	0.0520	0.0669
wR_2	0.1169	0.1311	0.1660
R indices (all data)			
R_1	0.0829	0.0726	0.0968
wR_2	0.1353	0.1469	0.1893
Largest diff. Peak and hole	0.743 and -0.495 e. Å^{-3}	0.965 and -0.979 e.Å^{-3}	0.610 and -1.185 e. Å^{-3}
CCDC	1523770	1523771	1523772

Table 2

Important bond distances (Å) and bond angles (°) in complexes **1**, **6**, and **7.**

	1 (H)	**6** (Me)	**7**(Et)
Cu –O1	1.9498(16)	1.9454(18)	1.953(2)
Cu–N3	1.9493(19)	1.9641(18)	1.955(3)

ACCEPTED MANUSCRIPT

Cu–S1	2.3174(7)	2.2577(7)	2.2579(9)
Cu–$N_{(eq)}$	2.013(2) (N4)	2.0305(19)(N5)	2.009(3)(N4)
Cu–$N_{(ax)}$	2.189(2) (N5)	2.3086(19)(N4)	2.217(3)(N5)
O1-Cu-$N_{(ax)}$	100.37(8) (N5)	91.17(7)(N4)	99.92(11)(N5)
O1-Cu-S1	151.13(6)	164.70(6)	150.82(9)
O1-Cu-$N_{(eq)}$	88.95(7)(N4)	88.52(7)(N5)	89.11(10)(N4)
N3-Cu-S1	83.66(6)	84.84(6)	85.25(7)
N3-Cu-O1	92.64(7)	93.21(7)	92.97(10)
N3-Cu- $N_{(eq)}$	176.86(8)(N4)	172.53(8)(N5)	175.25(10)(N4)
$N4_{(eq)}$-Cu- $N5_{(ax)}$	78.24(8)	76.40(7)	77.59(10)
τ value	0.428	0.131	0.407

$N_{ax} = N_{axial}$; $N_{eq} = N_{equatorial}$

3.3. ESR spectroscopy

The X-band ESR spectra of microcrystalline samples of copper(II) complexes **1-12** have been recorded and the important parameters are listed in Table 3. Figures **4-9** depict the representative ESR spectra of these complexes which unequivocally confirm the presence of a divalent oxidation state ($3d^9$) of copper in all these complexes. Probably, due to the distortion in geometry, all ESR signals expected in the parallel and the perpendicular regions involving coupling from ^{63}Cu (I = 3/2) nucleus are not observed. The ESR signals observed in the two regions are either partially resolved or merge into one another making it difficult to analyze the ESR spectra in the context of electron spin-nuclear spin coupling. However, an attempt is made to calculate A, g and G parameters for these complexes and infer the possible information from the spectra obtained (Table 3). Complex **1** has shown inverted axial ESR spectrum which is interesting and g parameters are : g_{II} =2.026 ; $g_{\perp}$ = 2.154 (Fig. 4) which suggests dz^2 ground state. Complexes **2, 4-7, 9** and **11** have shown axial ESR spectra (Figs 5-8) with g parameters in the trend : gII > g⊥ > 2 which implies that d_{x2-y2} is the ground state of copper(II) in these complexes [67, 68]. Complexes **3**, **10** and **12** have shown rhombic spectra (Figs. 8 and 9) and their g_1, g_2, g_3 values calculated are : **3**, 2.196, 2.082 2.026; **10**, 2.110, 2.050, -; **12**, 2.198, 2.085 and 2.030. Finally complex **8** has shown an isotropic spectrum suggesting symmetrical

ACCEPTED MANUSCRIPT

environments (Fig. 4) with g_{iso} = 2.083. The exchange interaction between copper centers in the polycrystalline compound is revealed by the geometric parameter G, which is calculated using the equation, $G = g_{II}-2.003/g_{\perp}-2.003$. The G values calculated for complexes **2**, **4-7, 9, 11** fall in the range, 2.65 to 4.04 and as for most of complexes G < 4, it shows considerable exchange interaction in the solid complexes [67, 68].

Table 3

ESR data of complexes **1-12**

Complex	g-values		g_{iso}	G
1	2.026(g_{II})	2.154($g_{\perp}$)	2.111	0.15
2	2.191(g_{II})	2.052($g_{\perp}$)	2.098	3.67
3	g_1 = 2.196, g_2 = 2.082, g_3 = 2.026		2.101	-
4	2.186(g_{II})	2.072($g_{\perp}$)	2.110	2.65
5	2.197(g_{II})	2.064($g_{\perp}$)	2.108	3.18
6	2.195(g_{II})	2.053($g_{\perp}$)	2.101	3.76
7	2.173(g_{II})	2.065($g_{\perp}$)	2.101	2.74
8	g = 2.083		2.083	-
9	2.194(g_{II})	2.050($g_{\perp}$)	2.098	3.82
10	g_1 = 2.110,	g_2 = 2.050	2.080	-
11	2.193(g_{II})	2.050($g_{\perp}$)	2.097	4.04
12	g_1 = 2.198 , g_3 = 2.030	g_2 = 2.085	2.104	-

ACCEPTED MANUSCRIPT

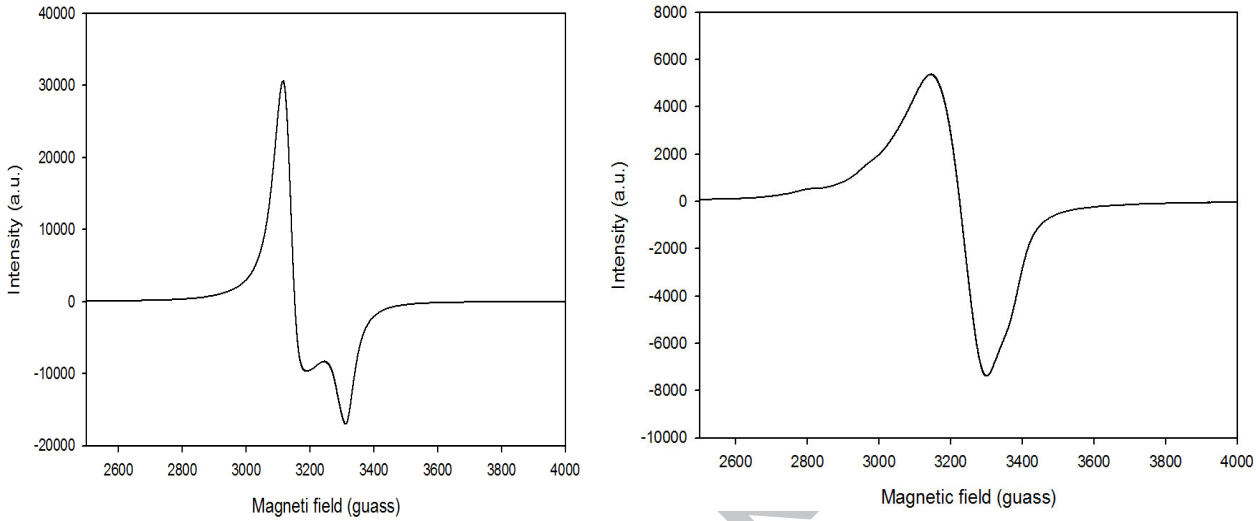

1 **8**

Fig. 4. The X-band ESR spectra of [Cu(κ^3-O,N^3,S-5-NO_2-stsc-N^1H_2)(κ^2-N,N-dm-bipy)] (**1**) and [Cu(κ^3-O,N^3,S-5-NO_2-stsc-N^{1}HEt)(κ^2-N,N-dm-phen] **(8)**.

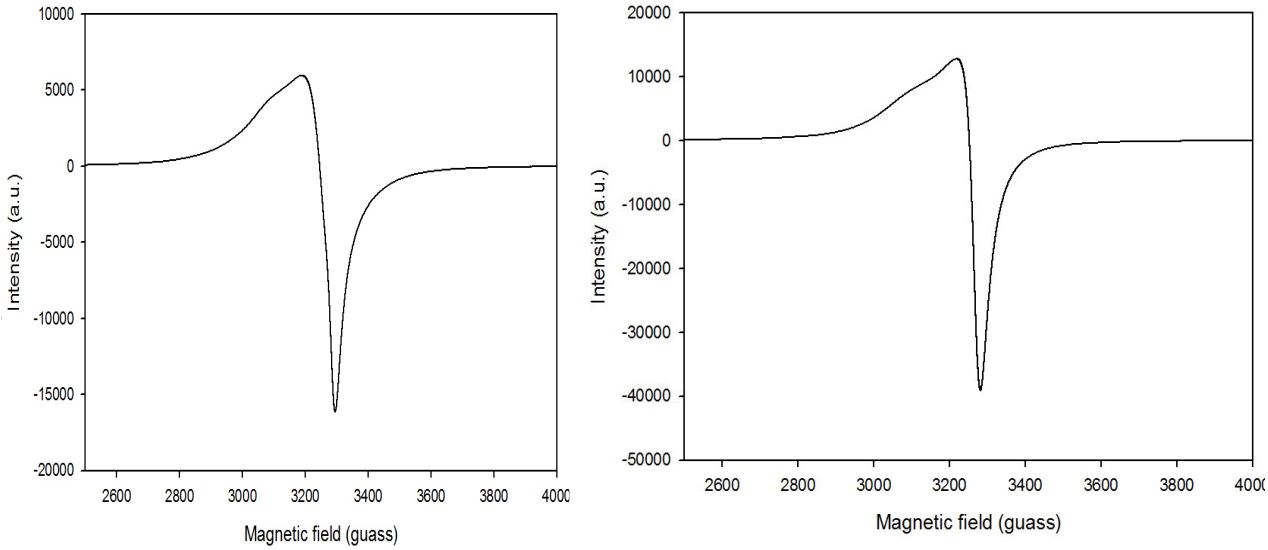

ACCEPTED MANUSCRIPT

4 **5**

Fig. 5. X-band ESR spectra of [Cu(κ^3-O,N^3,S-5-NO_2-stsc-N^{1}HMe)(κ^2-N,N-dm-bipy)] (**4**) and [Cu(κ^3-O,N^3,S-5-NO_2-stsc-N^{1}HMe)(κ^2-N,N-dm-phen] **(5)**.

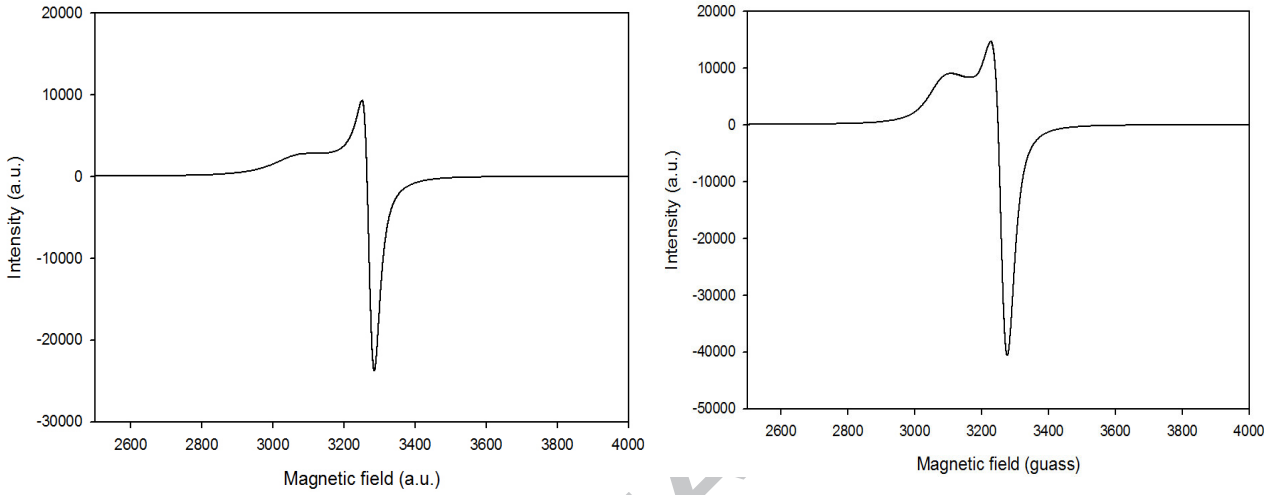

6 **7**

Fig.6. The X-band ESR spectra of [Cu(κ^3-O,N^3,S-5-NO_2-stsc-N^{1}HMe)(κ^2-N,N-tm-phen]·H_2O (**6**) and [Cu(κ^3-O,N^3,S-5-NO_2-stsc-N^{1}HEt)(κ^2-N,N-dm-bipy)]·CH_2Cl_2 **(7)**

ACCEPTED MANUSCRIPT

ACCEPTED MANUSCRIPT

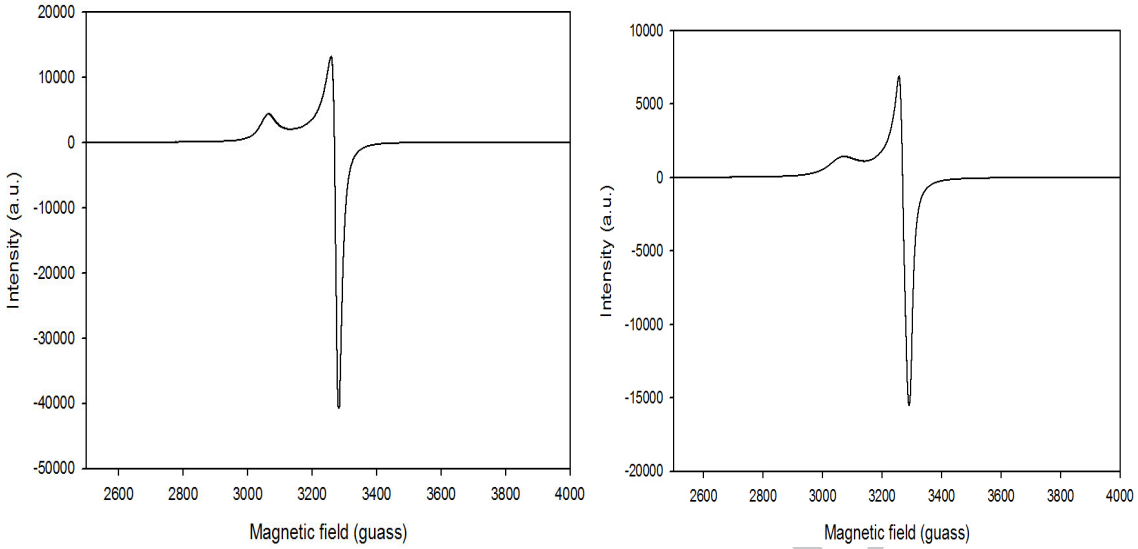

2 **9**

Fig. 7. [Cu(κ^3-O,N^3,S-5-NO_2-stsc-N^{1}H$_2$)(κ^2-N,N-2, 9-Me_2-phen] (**2**) and and [Cu(κ^3-O,N^3,S-5-NO_2-stsc-N^{1}HEt)(κ^2-N,N-tm-phen] (**9**)

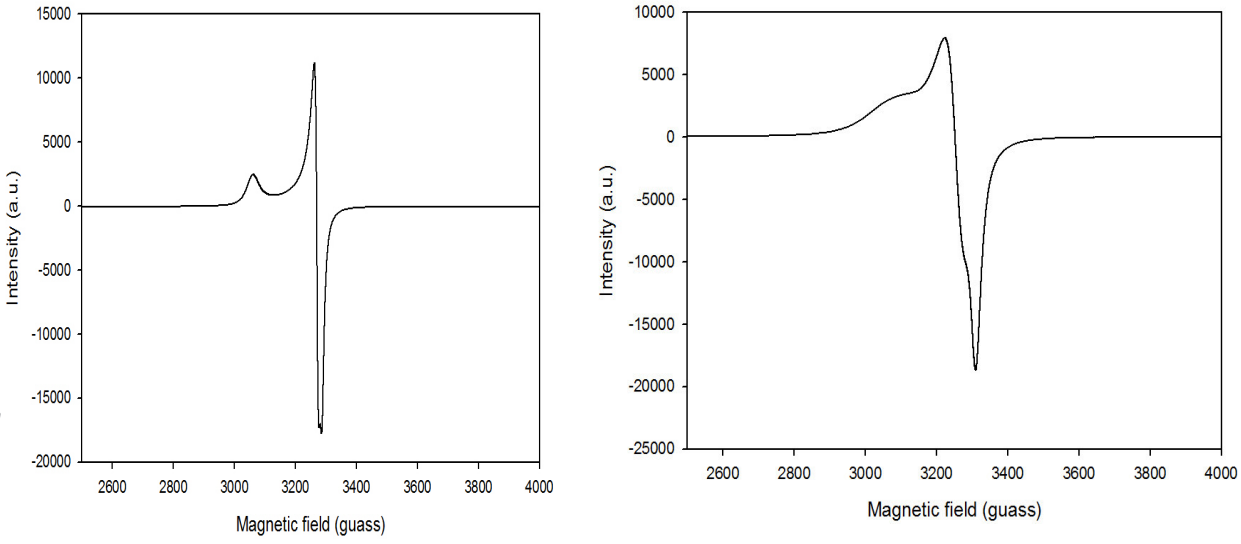

11 **3**

Fig.8. The X-band ESR spectra of [Cu(κ^3-O,N^3,S-5-NO_2- stsc-N^{1}HPh)(κ^2-N,N-dm-phen)] (**11**)

ACCEPTED MANUSCRIPT

and [Cu(κ^3-O,N^3,S-5-NO$_2$-stsc-N^{1}H$_2$)(κ^2-N,N-tm-phen]·CH$_3$OH (**3**)

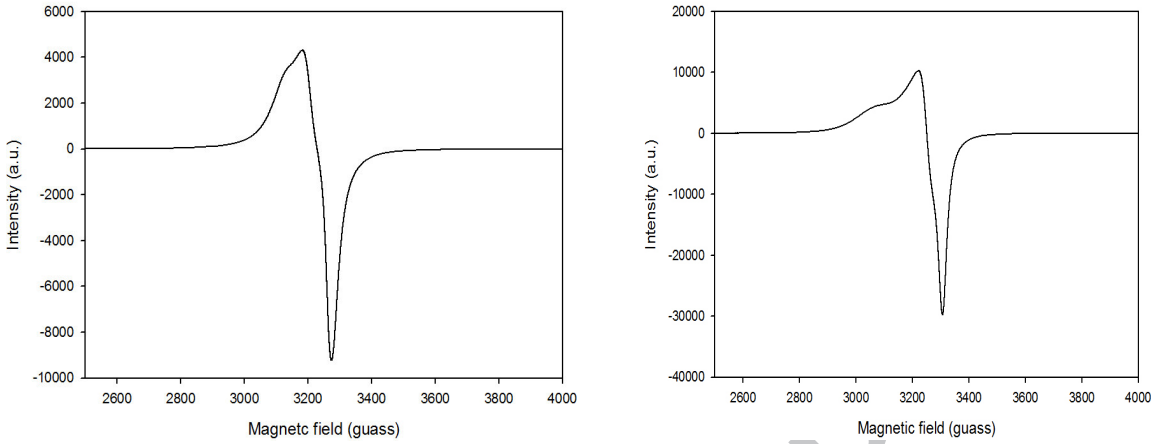

10 **12**

Fig.9. The X-band ESR spectra of [Cu(κ^3-O,N^3,S-5-NO$_2$- stsc-N^{1}HPh)(κ^2-N,N-dm-bipy] **(10)** and [Cu(κ^3-O,N^3,S-5-NO$_2$- stsc-N^{1}HPh)(κ^2-N,N-tm-phen)] **(12)**.

3.4. ESI Mass Studies

The ESI-mass studies of complexes have been carried out primarily to determine the molecular ion formation and confirm the molecular structures. Complexes (**1-7, 9- 11**) have shown the molecular ions, [Cu(ONS-L)(NN-L')+H]$^+$, which are listed in the experimental section. In addition, complexes **1**, **4-7** and **9** have shown the formation of dimeric species, [Cu$_2$(ONS)$_2$(NN)$_2$+H]$^+$ (Chart 4) (ONS- a thio-ligand; N,N- dm-bipy, dm-phen and tm-phen Lewis bases). Representative isotopic pattern and mass spectral peaks of both the species shown by complex **4** are displayed in Figs.10 and 11 (See supporting information for ESI-mass details – Figures **1S** to **25S**).

ACCEPTED MANUSCRIPT

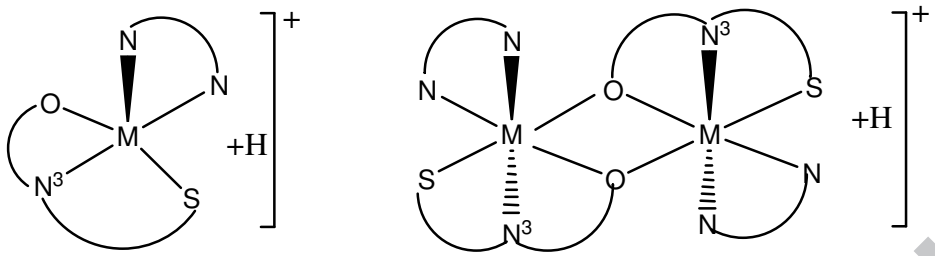

1-7, 9-11

$[Cu(ONS)(NN)+H]^+$

1, 4-7, 9

$[Cu_2(ONS)_2(NN)_2+H]^+$

Chart 4: Different species identified from ESI-mass study

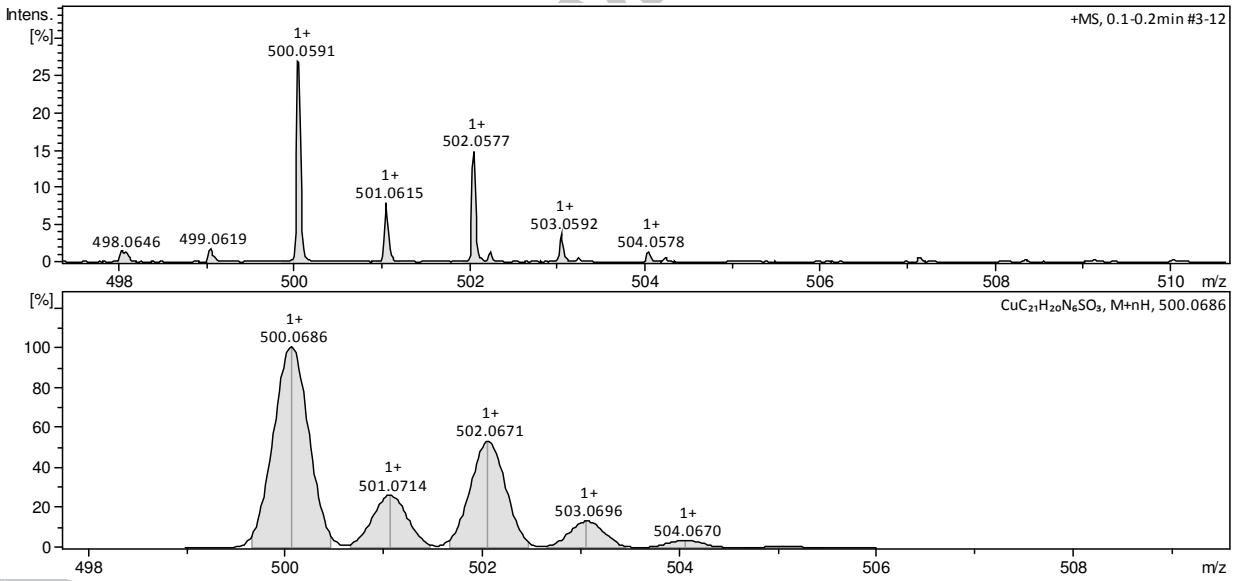

Fig. 10. ESI-mass peak due to molecular ion, $[Cu(5\text{-}NO_2\text{-}stsc\text{-}N^1HMe)(4,4'\text{-}Me_2\text{-}bipy)+ H]^+$ (m/z = calcd, 500.07, obsd. 500.06) with isotopic pattern (complex **4**).

ACCEPTED MANUSCRIPT

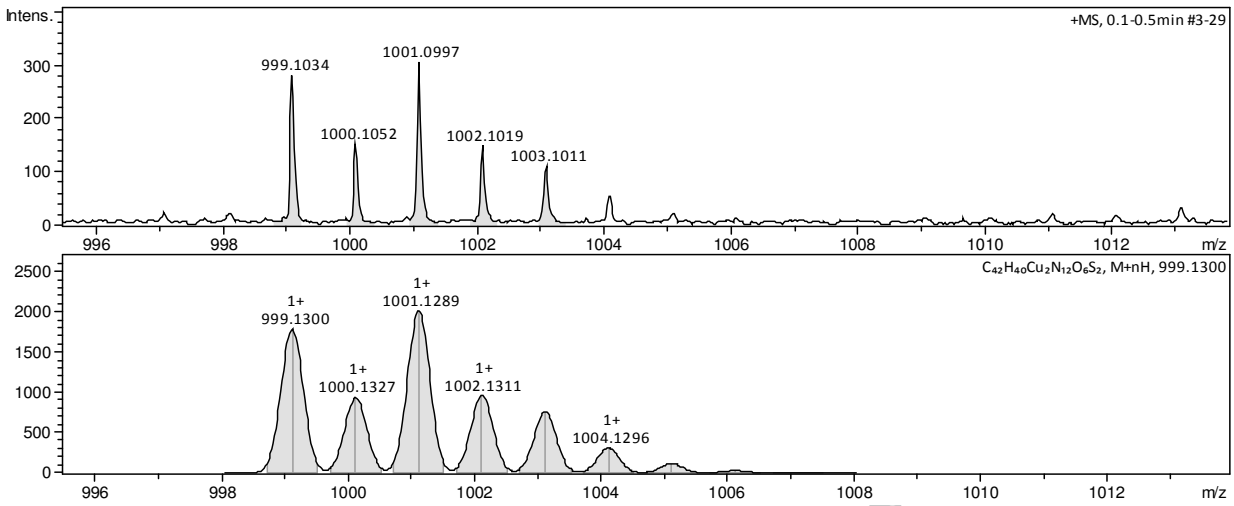

Fig.11. ESI-mass peak of dimeric $[Cu_2(5\text{-}NO_2\text{-}stsc\text{-}N^1HMe)_2(4,4'\text{-}Me_2\text{-}bipy)_2+ H]^+$ (m/z = calcd, 999.13, obsd. 999.10) with isotopic pattern (complex **4**).

3.5. Electronic absorption and fluorescence spectroscopy

The electronic absorption spectra of 10^{-3} M solutions of complexes **1-12** in DMSO have shown low intensity, broad d-d electronic absorption bands in the range, λ_{max} = 591-605 nm, attributed to the presence of copper(II). The 10^{-4} M solutions showed electronic spectral bands in the region, 277-287 nm and are assigned to $\pi \rightarrow \pi^*$ transitions. Bands in the region, 330-333 nm are assigned to $n \rightarrow \pi^*$ transitions (intra-ligand) and bands in the region, 398-406 nm are due to MLCT transitions [60-63, 69] (see experimental for more details). The electronic spectra are displayed in Figures.13-16.

ACCEPTED MANUS

ACCEPTED MANUSCRIPT

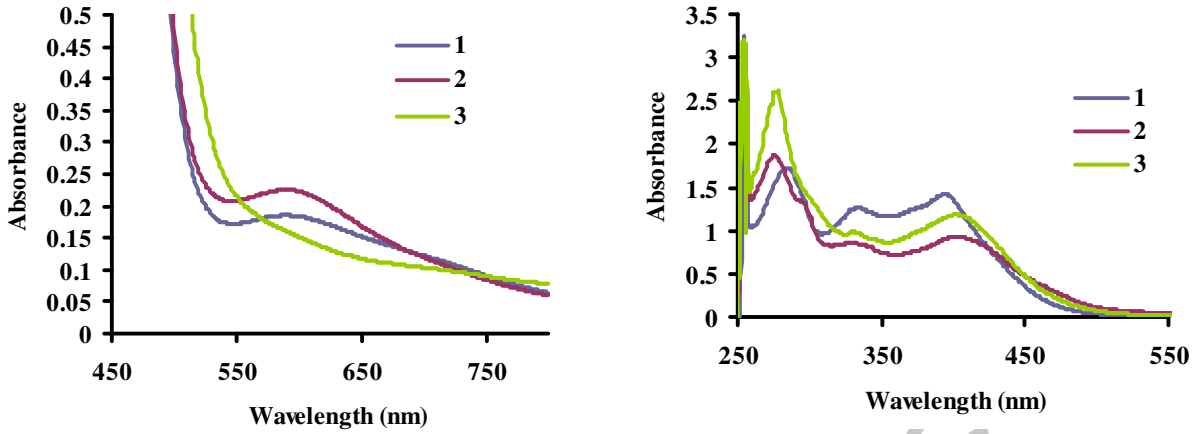

(a) [10^{-3}] M solutions (b) [10^{-4}] M solutions

Fig. 13. UV-Vis spectra of [Cu(κ^3-O,N^3,S-5-NO_2-stsc-N^1H_2)(κ^2-N,N-L')] (L' = dm-bipy **1**; dm-phen **2**; tm-phen **3**

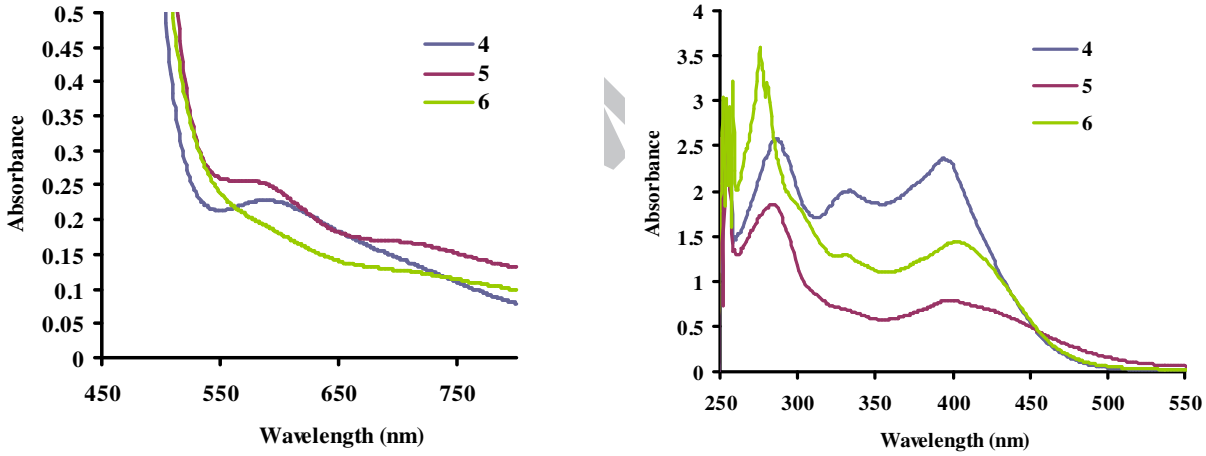

(a) [10^{-3}] M solutions (b) [10^{-4}] M solutions

Fig. 14. UV-Vis spectra of [Cu(κ^3-O,N^3,S-5-NO_2-stsc-N^{1}HMe)(κ^2-N,N-L')])] (L' = dm-bipy **4**; dm-phen **5,** tm-phen **6**)

ACCEPTED MANUSCRIPT

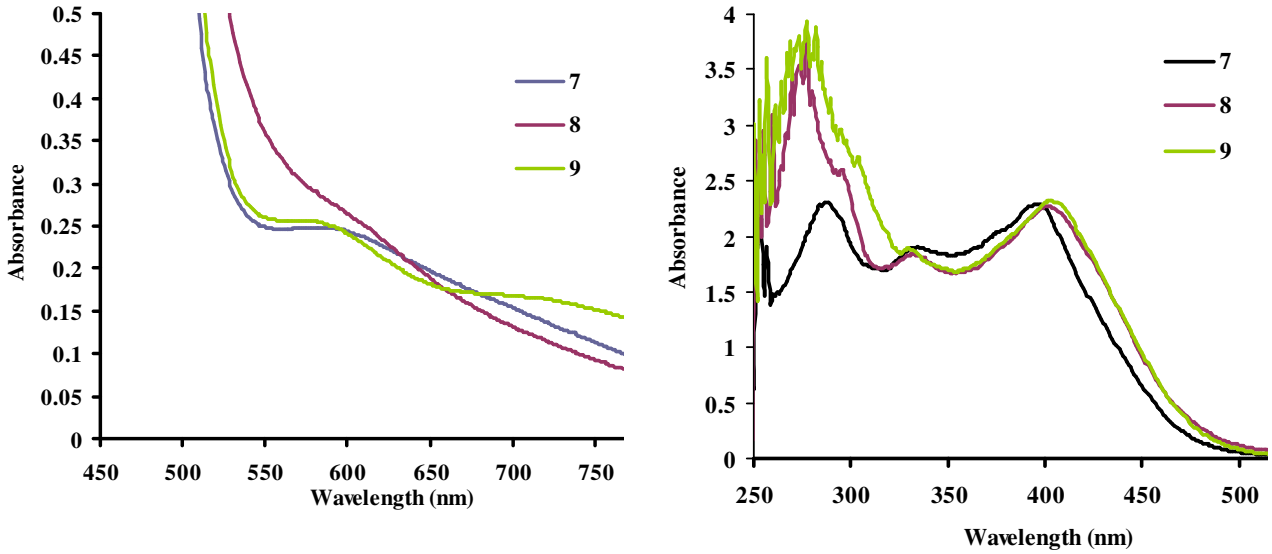

(a) [10^{-3}] M solutions (b) [10^{-4}] M solutions

Fig. 15. UV-Vis spectra of [Cu(κ^3-O,N^3,S-5-NO$_2$-stsc-N^{1}HEt)(κ^2-N,N-L')])] (L' = dm-bipy **7**; dm-phen **8,** tm-phen **9**)

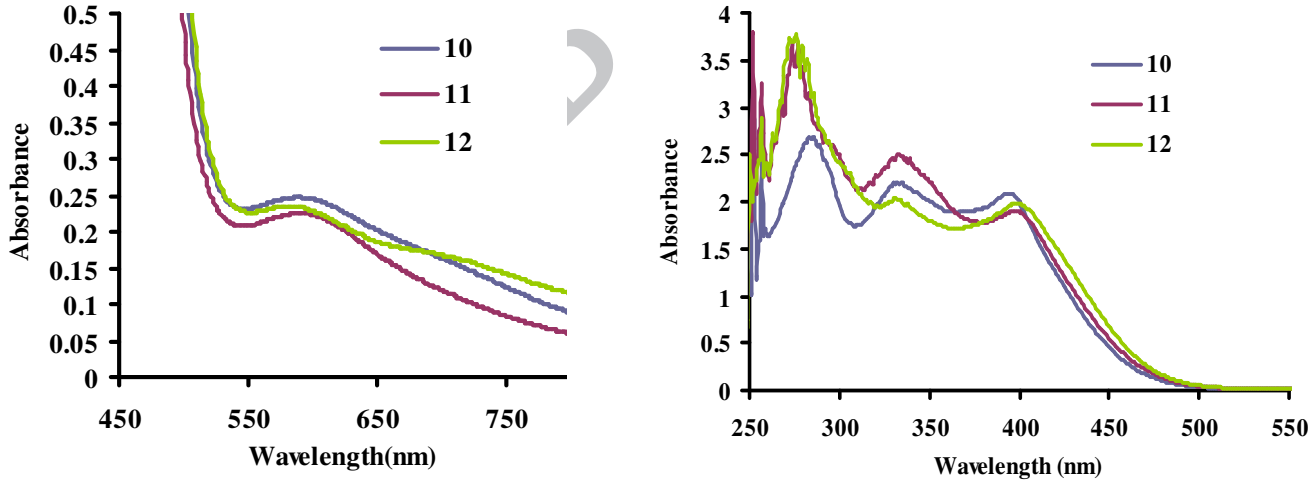

(a) [10^{-3}] M solutions (b) [10^{-4}] M solutions

Fig. 16. UV-Vis spectra of [Cu(κ^3-O,N^3,S-5-NO$_2$-stsc-N^{1}HPh)(κ^2-N,N-L')])] (L' = dm-bipy **10**; dm-phen **11,** tm-phen **12**)

ACCEPTED MANUSCRIPT

These complexes have shown fluorescence with λ_{max} at 433-437 nm corresponding to the excitation wavelength, λ_{ex} = 320 nm (Fig. 17). It may be noted that complexes with methyl substituted phen complexes **2**, **3**, **5**, **6**, **8**, **9**, **11** and **12** displayed more intense fluorescent bands (Fluorescence Intensity, F.I. = 110-135 a.u.) in comparison to methyl substituted bipy complexes **1**, **4**, **7** and **10** (F.I. = 90 a.u.; Fig.17). The difference in fluorescence intensity may be attributed to the fact that there occurs more conjugation in complexes with phen as a co-ligand than that in complexes with bipy as a co-ligand. It may also be noted that fluorescence intensity decreases when the R^3 group at N^1 nitrogen of thio-ligand changes from H to Ph. The fluorescence intensity of complexes **1-12** are in the range, 90-135 a.u., which is lower than that shown by unsubstituted bipy/phen complexes (180-270 a.u.) [52]. The difference is attributed to the inductive effect of an electronic withdrawing -NO_2 group which decreases the electron density on the complex and hence decreases the fluorescence intensity.

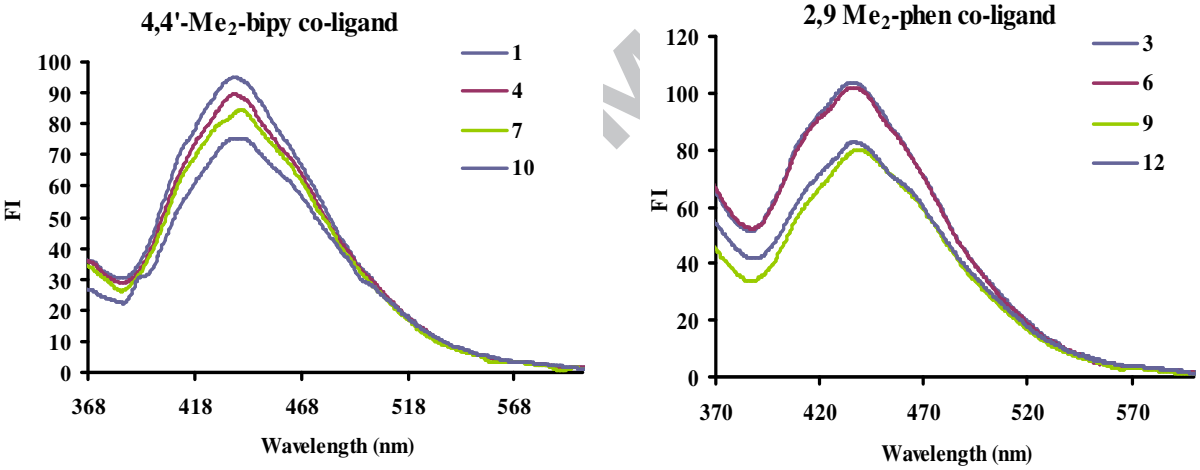

ACCEPTED MANUSCRIPT

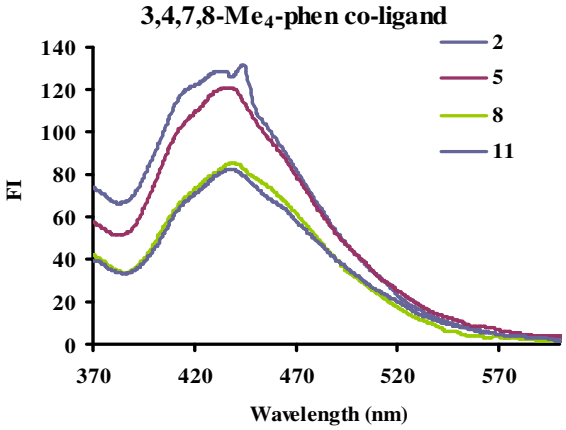

Fig. 17. Fluorescence spectra of complexes **1-12** {λ^{em} = 433 (**1**), 434 (**2**), 436 (**3**), 436 (**4**), 434 (**5**), 435 (**6**), 440 (7), 436 (**8**), 439 (**9**), 438 (**10**), 436 (**11**), 437 (**12**) nm; λ^{ex} = 320 nm}.

3.6. Antimicrobial activity-zone of inhibition

Table 4 lists the zone of inhibition data which is a measure of antimicrobial activity of copper(II) complexes with 5-nitro-salicylaldehyde-N^1-substitutedthiosemicarbazones, [Cu(κ^3-O,N^3,S-5-NO_2-stsc-N^1HR^3) -(κ^2-N,N-L')] (R^3 = H **1-3**, Me **4-6**, Et **7-9**, Ph **10-12**; N, N- L' = dm-bipy, **1**, **4**, **7**, **10**; dm-phen, **2**, **5**, **8**, **11** and tm-phen, **3**, **6**, **9**, **12**). Complexes **1**, **5**, **6**, **7** and **10** have shown antimicrobial activity ranging from 18-24 mm zone of inhibition (zoi) against methicillin resistant *staphylococcus aureus* (MRSA), while other complexes (**2**, **3**, **4**, **8** , **9**, **11** and **12**) showed very low activity (13-17 mm zoi). This activity is important as the commercially available Gentamicin was found to be inactive against the MRSA bacterial strain. As regards *Staphylococcus aureus,* complexes **1**, **4**, **5, 7, 10** and **12** exhibited activity in the range, 24-28 mm zoi which falls in the range of activity shown by Gentamicin (25 mm zoi); the activity of other complexes for this bacterial strain was less (16-22 mm zoi). Likewise, the activity of **1**, **5, 6** and **10** against *Klebsiella pneumoniae* is either close or higher (26-35 mm zoi) than the activity of Gentamicin (32 mm zoi); other complexes (**2-4,7-9,11 and 12**) showed lower activity(18-24 mm zoi). The activity against *Shigella flexneri* was shown only by complex **5** (18 mm zoi) close to that of Gentamicin (17 mm zoi). In the case of *Selmonella typhimurium*, several complexes (**1-7, 10-12**) exhibited antimicrobial activity in the range, 20-33 mm zoi and

ACCEPTED MANUSCRIPT

(cf. Gentamicin with 20 mm zoi). The highest activity against yeast, *Candida albicans* was shown by complex **5** with zoi of 31 mm, close to that of commercial Amphotericin (34 mm zoi); other complexes showed low activity (15-22 mm zoi).

Table 4

Antimicrobial activity[a,b,c] of complexes **1**-**12** (zone of inhibition)

Complex No.(R^3)	*MRSA*	*S. aureus*	*K. pneumoniae*	*S. flexneri*	*S. typhimurim*	*C. Albicans*
[Cu(κ^3-O,N^3,S-5-NO_2-stsc-N^1HR)(κ^2-N,N-dm-bipy)]						
1 (H)	18	26	26	N.A	28	22
4 (Me)	17	24	22	N.A	23	20
7 (Et)	19	26	24	N.A	26	21
10 (Ph)	18	24	26	N.A	26	22
[Cu(κ^3-O,N^3,S-5-NO_2-stsc-N^1HR)(κ^2-N,N-dm-phen)]						
2 (H)	15	16	18	N.A	23	17
5 (Me)	24	28	35	18	33	31
8 (Et)	15	21	21	N.A	18	18
11 (Ph)	13	20	21	N.A	23	20
[Cu(κ^3-O,N^3,S-5-NO_2-stsc-N^1HR)(κ^2-N,N-tm-phen)]						
3 (H)	13	17	18	N.A	20	17
6 (Me)	18	22	26	N.A	25	22
9 (Et)	13	18	18	N.A	15	15
12 (Ph)	17	24	22	N.A	22	19
Gentamicin[d]	N.A	25	32	17	20	-
Amphotericin[e]	-	-	-	-	-	34

[a)] All measurements are in mm diameter of the inhibition zone (N.A indicates no activity); [b)] The standard deviation varied in the range 0-1 based on three readings; [c)] Studies were made in DMSO; [d,e)] Commercially available anti-microbial agents. [d)] Gentamicin acts as positive control against bacteria (*MRSA*, *S. aureus, K. pneumoniae, S. flexneri, S. typhimurium*) and [e)] Amphotericin acts as positive control against yeast (*Candida albicans*).

ACCEPTED MANUSCRIPT

Minimum inhibitory concentration (MIC) and cyctotoxicity

It can be seen from Table 5 that several complexes were active at a minimum inhibitory concentration (MIC) of 5-7 μg/mL {*Staphylococcus aureus:* **1**, **5**, **7**; *Klebsiella pneumoniae*: **1**, **5**, **7, 9, 10**; *Selmonella typhimurium*; **1**, **5**, **7**, **9**, **10**}, MIC of 10 μg/mL {*Staphylococcus aureus*: **8**, **9**, **11**; *Klebsiella pneumoniae*: **4**, **11**, **12**; *Selmonella typhimurium:* **3**, **12**; *Candida albicans*: **1**, **4**, **7**, **9-12**} and MIC of 50 μg/mL {methicillin resistant *staphylococcus aureus*: **5**; *Staphylcoccus aureus:* **4**, **10**, **12**; *Selmonella typhimurium*; **2**, **4**, **11**}. Further, MIC of 750-1000 μg/mL was required for methicillin resistant *staphylococcus aureus*: **1**, **2**, **4, 7-10, 12,** *Staphylococcus aureus*: **2**, **3**, **6**; *Klebsiella pneumoniae:* **2**, **3**, **6, 8**; *Shigella flexneri:* **5** and *Selmonella typhimurium:* ***6, 8***; *Candida albicans*: **2**, **3**, **6**, **8**. All these complexes were further tested for cellular toxicity testing using sheep blood cells and it has been observed that the viability of living cells was very low and thus cellular toxicity of these complexes is high. In comparison, copper(II) complexes of the title ligands with un-substituted bipy/phen complexes displayed low cellular toxicity[52].

Table 5

Minimum Inhibitory concentration (MIC in μg/mL) of copper (II) complexes, **1-12**

Complex No.(R^3)	*MRSA*	*S. aureus*	*K. pneumoniae*	*S. flexneri*	*S. typhimurium*	*C. Albicans*
[Cu(κ^3-O,N^3,S-5-NO_2-stsc-N^1HR)(κ^2-N,N-dm-bipy)]						
1 (H)	750	7	7	N.A	7	10

ACCEPTED MANUSCRIPT

4 (Me)	750	50	10	N.A	50	10
7 (Et)	750	7	5	N.A	7	10
10 (Ph)	750	50	7	N.A	7	10
[Cu(κ^3-O,N^3,S-5-NO$_2$-stsc-N^{1}HR)(κ^2-N,N-dm-phen)]						
2 (H)	1000	750	750	N.A	50	750
5 (Me)	50	7	5	750	5	5
8 (Et)	1000	10	1000	N.A	750	750
11 (Ph)	-	10	10	N.A	50	10
[Cu(κ^3-O,N^3,S-5-NO$_2$-stsc-N^{1}HR)(κ^2-N,N-tm-phen)]						
3 (H)	-	750	750	N.A	10	750
6 (Me)	-	750	750	N.A	1000	1000
9 (Et)	750	10	7	N.A	7	10
12 (Ph)	750	50	10	N.A	10	10

4. Conclusion

The structures of these complexes are distorted square pyramidal and displayed intense fluorescence. The introduction of methyl substitution in the pyridyl rings of bipy/ phen co-ligands lowered fuorescence intensity *vis-à-vis* which was shown by similar complexes with the unsubstituted bipy/phen as co-liagnds [2]. ESI-mass spectral study supported the formation of molecular ions $[M + H]^+$ that supported the molecular structure of these complexes determined by X-ray crystallography. The antimicrobial activity of these complexes appeared to vary in the order : R = Me > Ph ~ Et > H. Among all the complexes investigated, complex [Cu(κ^3-O,N^3,S-5-NO$_2$-stsc-N^{1}HMe)(κ^2-N,N-dm-bipy)] **5** was most active against methicillin resistant *Staphylococcus aureus* (MRSA), *Staphylococcus aureus* (MTCC740), *Klebsiella pneumoniae* (MTCC109), *Shigella flexneri* (MTCC1457), *Salmonella typhimurium* (MTCC-439), and *Candida albicans* (MTCC227). These complexes are bactericidal / fungicidal and are toxic to living cells.

ACCEPTED MANUSCRIPT

Supporting Information

Appendix A. Supplementary data CCDC 1523770, 1523771 and 1523772 contains the supplementary crystallographic data for complexes **1**, **6** and **7,** respectively. These data can be obtained free of charge via http://www.ccdc.cam.ac.uk/conts/retrieving.html, or from the Cambridge Crystallographic Data Centre, 12 Union Road, Cambridge CB2 1EZ, UK; fax: (+44)1223-336-033; or e-mail: deposit@ccdc.cam.ac.uk. Supplementary data associated with this article can be found, in the online version, at http://dx.doi.org/.)

Acknowledgment

Financial assistance from the University Grant Commission (BSR, UGC); the Council of Scientific and Industrial Research (CSIR), New Delhi; Emeritus Scientist Grant [21(0904)/12-EMR-II] to TSL. JPJ acknowledges the NSF--MRI program (Grant No. CHE-1039027) for funds to purchase the X-ray diffractometer.

References

1 D. X. West, S. Padhye, and P. B. Sonawane, Struct. Bonding (Berlin), 76 (1991) 4-49.

2 D. X. West, A. E. Liberta, S. Padhye, R. C. Chilkate, P. B. Sonawane, A. S. Kumbhar, and R. G. Yerande, Coord. Chem. Rev., 123 (1993) 49-71.

3 J. S. Casas , M. S. Garcia-Tasende, and J. Sordo, Coord. Chem. Rev., 209 (2000) 197-261.

4 T. S. Lobana, R. Sharma, G. Bawa, and S. Khanna, Coord. Chem. Rev., 253 (2009) 977-1055.

5 T. S. Lobana, G. Bawa, A. Castineiras, R. J. Butcher, and M. Zeller, Organometallics, 27 (2008) 175-180.

6 J. Martinez, M. T. Pereira, I. Buceta, G. Alberdi, A. Amoedo, J. J. Fernandez, M. Lopez-Torres, and J. M. Vila, Organometallics, 22 (2003) 5581-5584.

ACCEPTED MANUSCRIPT

7 J. Dutta, S. Datta, D. K. Seth, and S. Bhattacharya, RSC Adv., (2012) 11751-11763.

8 J. Dutta, and S. Bhattacharya, RSC Adv., (2013) 10707-10721

9 S. Datta, D. K. Seth, R. J. Butcher, and S. Bhattacharya, Inorg. Chim. Acta, 377 (2011) 120–128.

10 R. K. Mahajan, T. P. S. Walia, Sumanjit, and T. S. Lobana, Talanta, 67 (2005) 755–759.

11 H. R. Fatondji, S. Kpoviessi, F. Gbaguidi, J. Bero, V. Hannaert, J. Quetin-Leclercq, J. Poupaert , M. Moudachirou, and G. C. Accrombessi, Med. Chem. Res.22 (2013) 2151–2162.

12 T. S. Lobana, P. Kumari, A. Castineiras, and R. J. Butcher, Eur. J. Inorg. Chem. (2013) 3557–3566.

13 T. S. Lobana, P. Kumari, Rekha Sharma, A. Castineiras, R. J. Butcher, T. Akitsu, and Y. Aritake, Dalton Trans. 40 (2011) 3219-3228.

14 T. S. Lobana, P. Kumari, R. J. Butcher, T. Akitsu, Y. Aritake, F. Fernandez, J. Perles, and M. C. Vega, J. Organomet. Chem., 701 (2012) 17-26.

15 T. S. Lobana, G. Bawa, and R. J. Butcher, Inorg. Chem. 47 (2008) 1488-1495.

16 T. S. Lobana, S. Indoria, M. Sharma, J. Nandi, J. A. Jassal, M. S. Hundal, and A. Castineiras, Polyhedron, 80 (2014) 34–40.

17 T. S. Lobana, S. Khanna, R. Sharma, G. Hundal, R. Sultana, M. Chaudhary, R. J. Butcher, and A. Castineira, Cryst. Growth Design 8 (2008) 1203–1212.

18 T. S. Lobana, S. Indoria, A. K. Jassal, H. Kaur, D. S. Arora, and J. P. Jasinski, Eur. J. Med. Chem. 76 (2014) 145-154.

19 P. D. Bonnitcha, A. L. Vajvere, J. S. Lewis, and J. R. Dilworth, J. Med. Chem., 51 (2008) 2985–2991

20 P. Wolohan, Y. Jeongsoo, J. W. Michael, and E. R. David, J. Med. Chem., 48 (2005) 5561-5569

ACCEPTED MANUSCRIPT

21 J. R. Dilworth, and R. Hueting, Inorg. Chim. Act, 389 (2012) 3–15.

22 R. L. Arrowsmith, P. A. Waghorn, M. W. Jones, A. Bauman, S. K. Brayshaw, Z. Hu, G. Kociok-Kohn, and T. L. Mindt, Dalton Trans., 40 (2011) 6238– 6252

23 S. I. Pascu, P. A. Waghorn, B. W. C. Kennedy, R. Arrowsmith, S. R. Bayly, J. R. Dilworth M. Christlie, R. M. Tyrrell, J. Zhong, R. M. Kowalczyk, D. Collison, P. K. Aley, G. C. Churchill, and F. I. Aigbirhio, Chem. Asian J. 2010, 5, 506 -519.

24 S. I. Pascu, P. A. Waghorn, T. D. Conry, B. Lin, H. M. Betts, J. R. Dilworth, R. B. Sim, G. C. Churchill, F. I. Aigbirhio, and J. E. Warren, Dalton Trans., 2008, 2107– 2110.

25 S. I. Pascu, P. A. Waghorn, T. D. Conry, H. M. Betts, J. R. Dilworth, G. C. Churchill, T. Pokrovska, M. Christlieb, F. I. Aigbirhio, and J. E. Warren, Dalton Trans., 2007, 4988 – 4997.

26 M. Christlieb, A. R. Cowley, J. R. Dilworth, P. S. Donnelly, B. M. Paterson, H. S. R. Struthers, and J. M. White, Dalton Trans., 2007, 327– 331.

27 R. I. Maurer, P. J. Blower, J. R. Dilworth, C. A. Reynolds, Y. Zheng, and G. E. D. Mullen, J. Med. Chem., 2002, 45, 1420-1431.

28 M. Christlieb, and J. R. Dilworth, Chem. Eur. J., 2006, 12, 6194 – 6206

29 K. A. Price, A. Caragounis, B. M. Paterson, G. Filiz, I. Volitakis, C. L. Masters, K. J. Barnham, P. S. Donnelly, P. J. Crouch, and A. R. White, J. Med. Chem., 2009, 52, 6606–6620.

30 a) M. C. Rodriguez-Argu, E. C. Lopez-Silva, J. Sanmartin, P. Pelagatti, and F. Zani, J. Inorg. Biochem., 2005, 99, 2231–2239. b) M. C. Rodríguez-Argüelles, P.Tourón-Touceda, R. Cao, A. M. García-Deibe, P. Pelagatti , C.Pelizzi and F. Zani, J. Inorg. Biochem. 2009, 103, 35–42.c) T. Rosu, E. Pahontu, S. Pasculescu, R. Georgescu, N. Stanica, A. Curaj, A. Popescu and M. Leabu , Eur. J. Med. Chem. 2010, 45, 1627–1634.

31 T. Rosu, A. Gulea, A. Nicolae, and R. Georgescu, Molecules, 2007, 12, 782-796.

32 (a) I. Babahan, F. Eyduran, E. P. Coban, N. Orhan, D. Kazar, and H. Biyik, Spectrochim. Acta Part A: Mol. Biomol. Spec., 2014, 121, 205–215; (b) A. Bacchi, M. Carcelli, P.

ACCEPTED MANUSCRIPT

Pelagatti, C. Pelizzi, G. Pelizzi, F. Zani, J. Inorg. Biochem. 1999, 75, 123–133.

33 A. G. Majouga, M I. Zvereva, M. P. Rubtsova, D. A. Skvortsov, A. V. Mironov, D. M. Azhibek, O. O. Krasnovskaya, V. M. Gerasimov, A. V. Udina, N. I. Vorozhtsov, E. K. Beloglazkina, L. Agron, L. V. Mikhina, A. V. Tretyakova, N. V. Zyk, N. S. Zefirov, A. V Kabanov, and O. A Dontsova, J. Med. Chem., 2014, 57, 6252–6258.

34 P. J. Jansson, P. C. Sharpe, P. V. Bernhardt, and D. R. Richardson, J. Med. Chem., 2010, 53, 5759-5769.

35 W. E. Antholine, J. M. Knight, and D. H. Petering, J. Med. Chem., 1976, 19, 339-341.

36 Z. Afrasiabi, E. Sinn, P. P. Kulkarni, V. Ambike, S. Padhye, D. Deobagakar, M. Heron, C. Gabbutt, C. E. Anson, and A. K. Powell, Inorg. Chim. Acta., 2005, 358, 2023–2030.

37 M. B. Ferrari, S. Capacchi, G. Pelosi, G. Reffo, P. Tarasconi, R. Albertini, S. Pinelli, and P. Lunghi, Inorg. Chim. Acta. 1999, 286, 134–141.

38 M. B. Ferrari, F. Bisceglie, G. Pelosi, P. Tarasconi, R. Albertini, and S. Pinelli, J. Inorg. Biochem., 2001, 87, 137–147.

39 B. M. Zeglis, V. Divilov, and J. S. Lewis, J. Med. Chem., 2011, 54, 2391–2398.

40 L. A. Saryan, E. Ankel, C. Krishnamurti, and D. H. Petering, J. Med. Chem., 1979, 22, 1218-1221.

41 E. A. Coats, S. R. Milstein, M. A. Pleiss, and J. A. Roesener, J. Med. Chem., 1978, 21, 804-809.

42 B. G. Patil, B. R. Havinale, J. M. Shallom, and M. P. Chitnis, J. Inorg. Biochem., 1989, 36, 107-113.

43 A. M. Thomas, A. D. Naik, M. Nethaji, and A. R. Chakravarty, Inorg. Chim. Acta., 2004, 357, 2315-2323.

44 V. I. Prisakar, V. I. Tsapkov, S. A. Buracheeva, M. S. Byrke, and A. P. Gulya, J. Pharm. Chem., 2005, 39, 30-32.

45 P. Bindu, M. R. P. Kurup, and T. R. Satyakeerty, Polyhedron, 1999, 18, 321-331.

46 R. P. John, A. Sreekanth, V. Rajakannan, T. A. Ajith, and M. R. P. Kurup, Polyhedron, 2004, 23, 2549-2559.

ACCEPTED MANUSCRIPT

47 D. X. West, Y. Yang, T. L. Klein, K. I. Goldberg, A. E. Liberta, J. V. Martinez, and R. A. Toscano, Polyhedron, 1995, 141, 1681-1693.

48 D. X. West, M. M. Salberg, G. A. Bain, and A. E. Liberta, Transition Met. Chem., 1997, 22, 180-184.

49 A. D. Naik, P. A. N. Reddy, M. Nethaji, A. R. Chakravarty, Inorg. Chim. Acta 349 (2003) 149-159.

50 M. Kurosu, P. N. K. Biswas, R. Dhiman, and D. C. Crick, J. Med. Chem., 2007, 50, 3973-3975.

51 Y. Hirokawa, H. Kinoshita, T. Tanaka, K. Nakata, N. Kitadai, K. Fujimoto, S. Kashimoto, T. Kojima, and S. Kato, J. Med. Chem., 2008, 51, 1991–1994.

52 T. S. Lobana, S. Indoria, H. Kaur, D. S. Arora, A. K. Jassal, J. P. Jasinski, RSC Adv. 5 (2015) 14916.

53 S. Indoria, T.S. Lobana, H. Kaur, D.S. Arora, A.K. Jassal, J.P. Jasinski, B.S. Randhawa, Polyhedron 107 (2016) 9–18.

54 S. Indoria, T.S. Lobana, Henna Sood, D.S. Arora, Geeta Hundal, J. P. Jasinski, New J. Chem. 40 (2016) 3642-3653

55 L. Palatinus, S. J. Prathapa and S. van Smaalen, J. Appl. Cryst. 45 (2012) 575-580.

56 L. Palatinus and A. van der Lee J. Appl. Cryst. 41 (2008) 975-984.

57 L. Palatinus and G. Chapuis,, J. Appl. Cryst., 40 (2007) 786-790.

58 G. M. Sheldrick, Acta Cryst. A64 (2008) 112-122.

59 O. V. Dolomanov, L. J. Bourhis, R. J. Gildea, J. A. K. Howard and H. Puschmann, J. Appl. Cryst., 42 (2009) 339-341.

60 G. M. Sheldrick, Acta Cryst. C71 (2015) 3-8.

61 L. Latheef, M. R. P. Kurup, Spectrochim. Acta. 70 (2008) 86.

ACCEPTED MANUSCRIPT

62 a) A. D. Naik, P. A. N. Reddy, M. Nethaji, A. R. Chakravarty, Inorg. Chim. Acta. 349 (2003) 149. b) E. B. Seena, M.R.P. Kurup, Polyhedron 26 (2007) 829.

63 A. M. Thomas, A. D. Naik, M. Nethaji, A. R. Chakravarty, Inorg. Chim. Acta. 357 (2004) 2315.

64 T. S. Lobana, P. Kumari, R. J. Butcher, J. P. Jasinski, J. A. Golen, Z. Anorg. Allg. Chem. 638 (2012), 1861.

65 R. P. John, A. Sreekanth, V. Rajakannan, T. A. Ajith, M. R. P. Kurup, Polyhedron 23 (2004) 2549.

66 A. W. Addison, T. N. Rao, J. Reedijk, J. Rijn, G. C. Verschoor, J. Chem. Soc. Dalton Trans. (1984) 1349.

67 A. Sreekanth, M. R. P. Kurup, Polyhedron 22 (2003) 3321.

68 V. Philip, V. Suni, M. R. P. Kurup, M. Nethaji, Polyhedron 24 (2005) 1133.

69 A. B. P. Lever, Inorganic electronic spectroscopy (second Edition) Elsevier, New York, 636 (1984).

ACCEPTED MANUSCRIPT

ACCEPTED MANUSCRIPT

Graphical abstract-pictogram

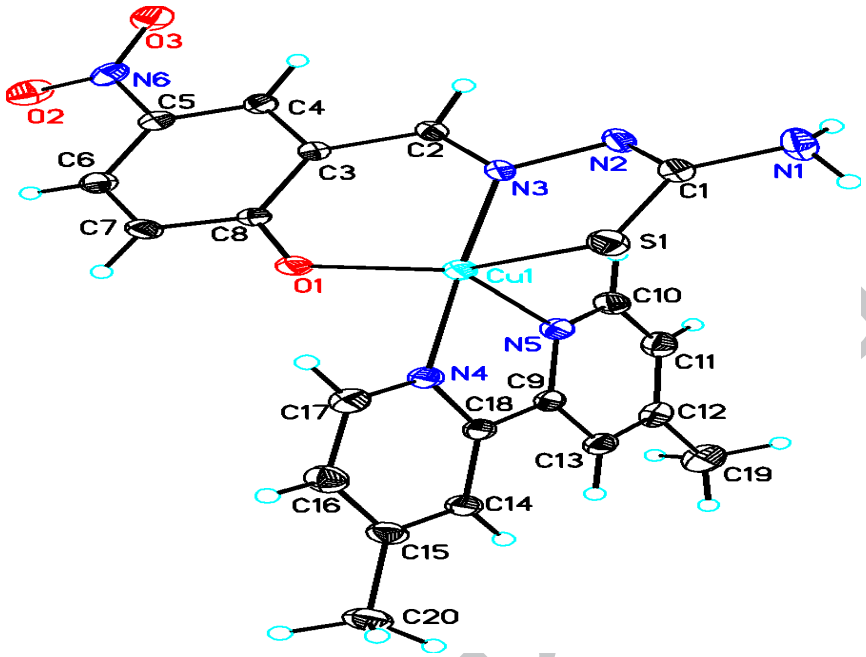

ACCEPTED MANUSCRIPT

ACCEPTED MANUSCRIPT

Graphical abstract –synopsis

Five coordinated copper(II) complexes of 5-nitro-salicylaldehyde-N-substituted thiosemicarbazones with methyl substituted 2,2-bipyridine and 1,10-phenanthrolines have shown bactericidal / fungicidal activity against methicillin resistant MRSA, *Staphylococcus aureus* (MTCC740), *Klebsiella pneumoniae* (MTCC109), *Shigella flexneri* (MTCC1457), *Salmonella typhimurium* (MTCC-439), and *Candida albicans* (MTCC227).

ACCEPTED MANUSCRIPT

ACCEPTED MANUSCRIPT

Highlights

1. Copper(II) complexes of 5-nitrosalicylaldehyde-N-substituted thiosemicarbazones are described
2. Molecular structures, ESI-mass and ESR spectroscopy make the focus of study
3. Antimicrobial activity of complexes with substituted bipyridines /phenanthrolines investigated.

ACCEPTED MANUSCRIPT